MULTI-SCALE DISCRETE FRAMELET TRANSFORM FOR GRAPH-STRUCTURED SIGNALS*

HUI JI†, ZUOWEI SHEN†, AND YUFEI ZHAO‡

Abstract. Graph-structured signal enables rich description of data defined in the domain with irregular structure, which has seen its rapid growth in many applications including social, energy, transportation, sensor, neuronal networks and many others. This paper aims at generalizing discrete framelet transform defined for regular grids in Euclidean space to finite undirected weighted graphs. By leveraging the intuition from classic framelet transform for signals on regular grids, we proposed an approach for constructing multi-scale undecimal framelet transform for signals defined on finite graphs with perfect reconstruction property. The proposed method is based on the definition of basic blocks involved in framelet transform, including graph shift operator, convolution and band-limited down/up sampling. These blocks enable a painless construction of a class of multi-level undecimal framelet transforms in vertex domain by directly calling wavelet filter banks of existing wavelet bi-frames and tight frames. The proposed discrete framelet transform on graphs keeps most desired properties of its counterpart on regular grids, and can see its usage in applications.

Key word. frame and tight frame, graph, signal processing

AMS subject classifications. 42A16, 42C40, 65T60

1. Introduction.

In recent years, we have witnessed a tremendous explosion of graph related data in a wide variety of scenarios. For example, sensor network deployed to measure physical entities such as temperature and radiation, brain imaging for measuring functional activities of biological network, analytics of online social network for mining social interactions, 3D depth cameras for understanding the scene environment. The structure of signals from these applications is no longer confined on uniform grids in Euclidean space. These signals are often intrinsically discrete and are defined on topologically complicated domains. Graph provides a very flexible model for encoding geometric properties of such signals. Often, the vertices of a graph represent signal sources and carry signal values. The edge weights of the graph capture the pairwise relationship between the vertices, e.g., geographical distance or biological connectivity. A graph structured signal is then defined as a function that assigns a value to each vertex. In other words, consider a graph $G = (\mathcal{V}, E, \omega)$ comprising a set of vertices $\mathcal{V} = \{v_j : j = 1, ..., |\mathcal{V}|\}$, a set of edges $E \subset \mathcal{V} \times \mathcal{V}$ and a weight function $\omega : E \to \mathbb{R}^+$. A graph G structured signal f is a signal defined on the vertices of graph G such that $f[j]$ denotes the signal value on the vertex j.

Graph-structured signals allow rich description of data defined in the domain with irregular structure, which is challenging for classic tools derived for data defined on regular grids in Euclidean space. Also, structure-agonistic transform is not optimal when being used for representing graph structured signals as key dependencies and topological properties of such signals are discarded. Therefore, in order to efficiently exploit graph structured signals, the transform for representing such signals needs to effectively treat the underlying graph structure. In recent years, adapting classic signal processing tools to signals defined on graphs has seen its significant interest in the communities. One fundamental challenge of representing graph structured signals is how to leverage the intuition from classical signal processing in Euclidean space on the design of discrete transforms,

*Submitted to the editors.

Funding: This work is supported by "the Fundamental Research Funds for the Central Universities", Nankai University (63191415) and Singapore MOE AcRF Tier 2 Grant (MOE2017-T2-2-156).

†Department of Mathematics, National University of Singapore (matjh@nus.edu.sg,matzuows@nus.edu.sg).

‡School of Mathematical Sciences, Nankai University (matzyf@nankai.edu.cn).

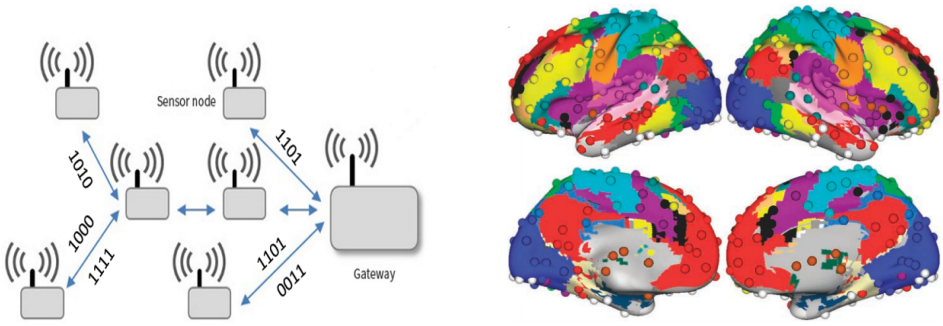

FIG. 1.1. *Illustration of graph-structured signals. Left: sensor network, right: Brain functional network [30]*

which can incorporate graph structure of signals and can be implemented with simplicity and efficiency.

1.1. Motivation. In last few decades, owing to its effectiveness on characterizing local discontinuities in a multi-scale manner, wavelet transform [12, 24] has been one fundamental tool in classic signal processing. With the prevalence of sparse approximation/representation related theories and algorithms, wavelet tight frame based redundant transforms also see their wide adoptions in many applications related to the processing of signals defined on equi-spaced grids. For example, translational-invariant wavelet transform [9] and spline framelet transform [13, 33] for audio and image processing.

There are several properties of wavelet/framelet transform that make it very appealing to signal processing, including

(i) Localized analysis of signals in time domain by only employing operators defined on the neighborhood of each point, which leads to effective characterizing of local discontinuities.
(ii) Multi-scale analysis of signals that enables the decomposition of a signal into a coarse channel that encodes the smooth components of the signal and multiple channels that encode the discontinuity details of the signal in multiple scales.
(iii) The *perfect reconstruction property* that enables the exact forward and backward process of a signal and its transform coefficients
(iv) The simple and efficient cascade algorithms for signal decomposition and reconstruction.

However, owing to the irregular structure of general graph, it is a challenging task to generalize discrete wavelet/framelet transform from equi-spaced grid to general graph, while keeping all desired properties of classic wavelet/framelet transforms listed above. In recent years, there has been an enduring effort to generalize wavelet-type transform from equispaced Euclidean grids to general graphs. Similar to the development of classic wavelet transform, the construction of wavelet-type transform can be roughly classified into vertex domain based approach [11, 40, 28, 41, 18, 31, 6, 7] and spectral domain based approach [10, 23, 19, 21, 36, 37, 39, 43, 14]. The majority of vertex domain based approaches are based on the construction of a tree graph that abstracts the graph with certain properties, e.g., the k-hop connectivity between the vertices. Such tree graphs are in parallel to the tree structure of multi-resolution analysis (MRA) in equispaced grids, and thus classic MRA-based wavelet transforms can be directly defined from tree graphs, which approximate the given graphs. Nevertheless, constructing a tree graph that keeps most information of a given general graph is a very challenging optimization problem. Often, a tree graph based abstraction

of a general graph can lead to undesired loss of important information. For instance, the shortest path distance of the graph for analyzing computer network traffic.

The spectral domain based approach is based on spectral structure of a graph, which is represented by the eigenvalues and eigenvectors of the graph Laplacian defined on the adjacent matrix of the graph. These eigenfunctions provide a spectral decomposition for signals on graph similar to discrete Fourier transform (DFT) for classic signals. As the convolution, one key operation in wavelet transform, can be expressed as diagonal multiplication in spectral domain, the generalization of classic wavelet transform can be naturally done in spectral domain. Nevertheless, the construction of wavelet transform in spectral domain also has its own issues. One is the localization of the transform in vertex domain. In contrast to vertex domain based construction, it is quite challenging to design transforms in spectral domain that running local operations in vertex domain, while keeping perfect reconstruction property. Indeed, most existing spectral domain based wavelet transforms either do not have good localization in vertex domain or do not have perfect reconstruction property. Also, existing spectral domain based wavelet transforms do not provide many choices, as they are specifically derived for certain examples of wavelet transform in equi-spaced grids.

1.2. Aim and the approach. This paper aims at generalizing classic discrete framelet transform to signals defined on undirected graphs. The discrete framelet transform proposed in this paper will leverage the intuition from classic framelet transform in Euclidean spaces such that it not only replicates classic framelet transform on equispaced grids, but also keeps those desired properties during the generalization, including multi-scale analysis, and perfect reconstruction property.

We take a new approach to construct discrete framelet transform for signals on undirected graphs. Different from those tree graph based constructions, the proposed approach is directly defined on the original graph without tree-structured abstraction. Different from those constructions in spectral domain, the proposed approach views the fundamental analogy between signal processing on equispaced grids and undirected graphs is on the definition of the shift (translation) operator, i.e., how the information propagates from one vertex to its neighbors. By taking the shift operator as the fundamental building block, it is very natural to introduce the discrete convolution on graph, which greatly facilitates the construction of framelet transform with two important properties: the localization in vertex domain and the perfect reconstruction property. Discrete Fourier transform is defined as the eigenvectors of the induced translation operator, which remains consistent with the existing spectral approach. Together with the introduction of up/down-sampling in spectral domain, the proposed approach generalizes the classic framelet transform from equispaced grids to undirected graphs.

The construction focuses on the design of undecimal framelet transform. Undecimal transform is also often called translation-invariant transform in signal processing. For a signal defined on an equispaced grid, owing to the inclusion of down-sampling operation, the standard decimal wavelet/framelet transform is not invariant to the shifts of the signal over the grid. That is, the wavelet/framelet coefficients of a signal after a shift are not the same as (up to a shift) its original counterpart. The sensitivity of framelet coefficients with respect to shifts is not desirable in many applications. In practice, undecimal wavelet/frame transforms are often more preferred than its decimal counterpart in signal/image recovery. For example, translation-invariant wavelet transform for signal/image denoising [9], undecimal spline framelet transform for many image recovery tasks including image inpainting, deconvolution, and volume data reconstruction [2, 42, 3, 4, 22].

The framelet transform constructed in this paper can see its potential applications in many problems related to the processing/analysis of graph-structured signals. For example, graph based

semi-supervised learning ([16, 18, 44]), analysis of fMRI data ([20]) and diagonosis of Alzheimer's Disease in neuro-imaging ([45]).

1.3. Organization. The paper is organized as follows. We first present the definition and algorithm of multi-scale un-decimal framelet transform for signals on undirected graphs. Then, a sufficient condition for guaranteeing the perfect reconstruction property of multi-scale framelet transform is established for both bi-frames and tight frames. Indeed, the proposed sufficient condition is closely related to the Mixed Extension Principle (MEP) for classic wavelet bi-frames and the Unitary Extension Principle (UEP) for classic wavelet tight frames. As a result, we have a painless construction of undecimal multi-level framelet transform for signals defined on graphs. For example, the filter banks associated with spline wavelet tight frames [13, 33] can be directly called for defining undecimal multi-level tight framelet transform on graphs. In summary, this paper present an approach to construct undecimal framelet transform for signals on graphs that leverages the properties of classic framelet transform for signals defined on equispaced grids.

In the remaining of the paper, Section 2 gave a brief review on related works in existing literature. Section 3 presented related mathematical preliminaries, including multi-level discrete framelet transform in Euclidean spaces and some basic concepts in graph theory. In Section 4, we gave the notion of shift operator and other fundamental operators in wavelet transform. Based on these key operators, we defined the multi-level framelet transform on undirected graph and discussed its perfect reconstruction property in Section 5. In Section 6, we demonstrated some examples of proposed discrete framelet transform on irregular graph. Finally, in Section 7, we concluded the paper.

2. Related work. In recent years, there have been an enduring research effort on defining and constructing wavelet-type transforms for signals on graph. In this section, we only give a brief review on those most related works, which either define and construct wavelet related transform in vertex domain or graph spectral domain.

The approach in vertex domain utilizes spatial features of graph to exploit local information in the neighborhood of each vertex, e.g. vertex connectivities and edge weights. Representative works include graph wavelets [11], lifting wavelets on graph [40, 28], and tree based construction of wavelet transforms [18, 6, 7, 31, 32]. Crovella and Kolaczyk [11] proposed localized graph wavelet transform for signals on unweighted graph, in which the wavelet function at scale j centered around each vertex is strictly supported in a j-hop disk, i.e. set of vertices whose shortest path distance from the center is less than or equal to j. Across different scales, the support of wavelet function varies with j, which makes the transform able to examine local differences of a set of measurements in a multi-scale fashion. However, the transform defined in [11] is not invertible in general. In the lifting wavelet transform for graph proposed in ([40, 28]), at each scale, the vertex set is partitioned into sets of even and odd vertices. Then similar to the standard lifting scheme, the coefficient on an odd (or even) vertex is computed using its own signal value and signal values on its neighboring even (or odd) vertices. In the process of even-odd splitting of vertices, partial graph information of each vertex is lost, owing to the irregular structure of general graphs. For example, the adjacent vertices are artificially allocated to the same parity, and thus partial information of the neighborhood of any vertex is discarded in such a process.

In [18, 7], the graph, either directed or undirected, is clustered by some general-purpose clustering algorithm into hierarchical tree, which has the same topological structure as classic MRA defined on equispaced grids. Thus, classic wavelet systems defined on equispaced grids can be generalized to the tree in a straightforward way. Based on such a concept, various multi-scale

wavelet-like transforms have been proposed in the past. For example, Haar wavelet on tree [18], and orthonormalized systems of tree polynomials [6, 7]. In [31, 32], an L-level tree (or generalized tree) is constructed based on the distances among data points, which essentially is a rooted L-partite graph. The decomposition operation is different from the classic one by adding an additional re-ordering process on low-pass (approximation) coefficients at each level, which shortens the path passing through the coefficient. As a result, the smoothness of low-pass coefficients is improved and high-pass wavelet coefficients have better sparsity degree. Nevertheless, these tree based construction schemes of wavelet transforms depend on the abstraction process that converts a general graph into a graph with tree structure, which is difficult to have an optimal approach that keeps most geometrical information of a general graph. Certain important information is likely to be discarded in such an abstraction, e.g. the connectivity among adjacent vertices.

A prominent approach of constructing wavelet-type transform on graph is done in graph spectral domain, i.e., the generalized discrete Fourier transform on graph. Representative works of such an approach include diffusion wavelets [10, 23, 1] and Laplacian-based transforms [19, 20, 21, 43, 14, 29, 35]. In these works, basic operators and multi-scale structure involved in wavelet transform are defined using spectral features, including the eigenvalues and eigenvectors of graph Laplacian matrix derived from the adjacency matrix of a graph. Coifman and Maggioni [10] introduced diffusion wavelets for multi-scale representation of signals on manifolds and graphs, in which the dilation operator involved in classic wavelet transform is replaced by a diffusion operator. At each scale, the dyadic power of diffusion operator is first applied on basis elements and the resulted functions are then down-sampled via a localized orthonormalization scheme to produce an orthonormal basis for the next coarse level. Then, the wavelet functions are constructed by collecting locally orthogonalizing atoms spanning the difference between two consecutive levels, which leads to an orthonormal wavelet-type transform on graph. It is further extended to bi-orthogonal diffusion wavelets [23] and diffusion wavelet packets in [1] for manifolds and graphs. However, it is indicated in [19] that the orthogonalization procedure in the construction of diffusion wavelets is quite complicated, and it obscures the relationship between diffusion operator and resulting wavelets.

Based on graph Laplacian [8], another type of spectral graph wavelet transforms is introduced in [19], which defines the shift, discrete convolution and dilation operators all in graph spectral domain, which is in parallel to the Fourier transform based expression of these operations in equispaced grids. The operators related to the scaling and wavelet functions are then defined using the generalized convolution, spectral scaling kernel and wavelet kernels dilated at different scales. Many consequent works follow such an approach, and the main difference lies in which spectral kernels are used to generate wavelet systems. For example, in [20, 21], tight wavelet frames are constructed by using Meyer-like wavelet and scaling kernels. Based on definition of the translation and warping in the graph spectral domain, spectral kernels are adapted in [43] to the distribution of graph Laplacian eigenvalues to yield spectrum-adapted tight graph wavelet frames. Another wavelet frame transform on graph is introduced in [14], which considered the construction of wavelet tight frames on both manifolds and graphs. In [14], the wavelet functions on manifold are generated from a refinable function and a filter bank that includes both refinement masks and wavelet masks. The filter bank is then used as the spectral kernels for generating systems on graph. It is shown in [14] that tight frame property of proposed quasi-affine systems (undecimal system) on manifolds, as well as associated discrete multi-level systems on graphs, is guaranteed by one of conditions in *unitary extension principle* [33, 13] for classic MRA-based wavelet tight frame in Euclidean space.

In comparison to vertex domain based transforms, graph Laplacian based wavelet-type transforms usually do not include down/up-sampling process, as how to meaningfully down-sample a

graph is not clear in general. For specific types of graph, particularly bipartite graph, the vertices can be divided into two dis-joint subsets such that there is no edge inside each subset. Such property allows a down-sampling process in parallel to its counterpart in equi-spaced grids. By consequentially decomposing a general graph into bi-partite subgraphs, a class of two-channel critically sampled orthonormal wavelet transforms are proposed in [29]. In [35], the down/up-sampling process is designed in the spectral domain via spectrum folding of frequencies. With such down/up-sampling approach, the two-channel graph Laplacian based (bi-)orhtogonal wavelet transform is constructed in [35].

Furthermore, since the atoms associated with the graph Laplacian based transforms are eigenvectors of the graph Laplacian, they are usually not localized in vertex domain. For computational efficiency, sometimes such transforms are approximated using Chebyshev polynomials of graph Laplacian (e.g. [19, 14]). When adopting Chebyshev polynomials approximation based computational scheme, the perfect reconstruction property of the original wavelet transform does not hold true anymore. The computation using Chebyshev polynomials indeed is parallel to the recent work on digital signal processing that defines convolution operations directly from the adjacency matrix.

The recent work on digital signal processing on graph ([36, 37, 38, 39]) is very related to wavelet-type transform on graph. The basic operations often seen in digital signal processing, including shift operator, discrete convolution, and frequency response, are also the fundamental operations involved in wavelet-type transforms. In [36, 37, 38, 39], the shift operator serves as basic building block to define convolution, Fourier transform, frequency responses and so on. The shift operator in these works is defined as the adjacency matrix of the graph, regardless directed or undirected graph. Such definition of shift operator on undirected graphs has its issues, as it can not replicate its classic counterpart on 1D equispaced grids with periodic boundary extension, i.e., a cyclic permutation matrix. In addition, some other ingredients and properties involved in wavelet transform are not discussed in these works, e.g. down/up sampling operations and perfect reconstruction property.

3. Preliminaries. We first give an introduction to the notations used in this paper. Throughout this paper, we use $\mathbb{Z}, \mathbb{Z}^+, \mathbb{R}, \mathbb{C}$ to denote the set of integers, positive integers, real-valued numbers and complex-valued numbers, respectively. For any $d \in \mathbb{Z}$, let $\mathbb{Z}^d$ denote the d-dimensional Euclidean space of integer numbers. For any $M \in \mathbb{Z}^+$, define $\mathbb{Z}_M := [-(M-1), M-1] \cap \mathbb{Z}$ and define $\mathbb{Z}_M^d := [-(M-1), M-1]^d \cap \mathbb{Z}^d = \mathbb{Z}_M \times \cdots \times \mathbb{Z}_M$. For any $x \in \mathbb{C}$, let x^* denote its complex conjugate. We denote the linear space of all sequences by $\ell(\mathbb{Z})$, and the linear space of all sequences with finite non-zero elements by $\ell_0(\mathbb{Z})$. For any sequence $f \in \ell(\mathbb{Z})$, its k-th element is denoted by $f[k]$. For a matrix $A \in \mathbb{C}^{M\times N}$, let A_j denote its j-th column, and $A_{k,j}$ the entry at its k-th row and j-th column. The conjugate transpose of a matrix A is denoted by A^*, and its inverse is denoted by A^{-1} if exists. Let I_N denote the $N \times N$ identity matrix. For matrix concatenation, semi-colons are used for adding elements in columns and commas are used for adding elements in rows. The cardinality of a finite set Ξ is denoted by $|\Xi|$.

3.1. MRA-based Wavelet tight (bi) frames. In this section, we give a brief introduction to multi-scale (or multi-level) discrete framelet transform for signals defined on equispaced Euclidean grids. Consider a Hilbert space H with inner product $\langle \cdot, \cdot \rangle$. A sequence $\{v_n\}_{n\in\mathbb{Z}} \subset H$ is called a *frame* if there exist two positive constant A, B such that

$$A\|f\|^2 \le \sum_{n\in\mathbb{Z}} |\langle f, v_n\rangle|^2 \le B\|f\|^2, \quad \forall\, f \in H.$$

The sequence $\{\widetilde{v}_n\}_{n\in\mathbb{Z}} \subset H$ is called its *dual frame* if

$$f = \sum_{n\in\mathbb{Z}} \langle f, v_n\rangle \widetilde{v}_n = \sum_{n\in\mathbb{Z}} \langle f, \widetilde{v}_n\rangle v_n, \quad \forall\, f \in H. \tag{3.1}$$

A frame $\{v_n\}_{n\in\mathbb{Z}}$ is called *tight frame* when $A = B = 1$. For a tight frame, one of its dual frames is the tight frame itself. A frame $\{v_n\}_{n\in\mathbb{Z}}$ and its dual $\{\widetilde{v}_n\}_{n\in\mathbb{Z}}$ are called *bi-frames* for H.

Multi-scale discrete framelet transform for signals defined on equi-spaced grids is derived from MRA-based wavelet frames for $L_2(\mathbb{R})$. Consider a refinable function $\phi \in L_2(\mathbb{R})$ with $\widehat{\phi}(0) = 1$ that satisfies

$$\phi(k) = 2\sum_{k\in\mathbb{Z}} h_0[k]\phi(2x - k),$$

for some finite sequence $h_0 \in \ell_0(\mathbb{Z})$, the so-called refinement mask of ϕ. The function ϕ admits a multi-resolution analysis (MRA) of $L_2(\mathbb{R})$, if the sequence of subspaces $\{V_n\}_{n\in\mathbb{Z}}$ defined by

$$V_n = \overline{\operatorname{span}\{2^{\frac{n}{2}}\phi(2^n - k)\}_{k\in\mathbb{Z}}}$$

satisfies

$$(1)\, V_n \subset V_{n+1}, \quad n \in \mathbb{Z}, \quad (2)\, \overline{\cup_n V_n} = L_2(\mathbb{R}), \quad (3)\, \cap_n V_n = \{0\}.$$

Define a set of framelets $\Psi = \{\psi_j\}_{j=1}^r$ as

$$\psi_j(\cdot) = 2\sum_{k\in\mathbb{Z}} h_j[k]\phi(2\cdot - k), \quad 1 \le j \le r.$$

Then, the UEP [33, 13] says that the corresponding wavelet (affine) system defined by

$$X(\Psi) = \{2^{n/2}\psi_j(2^n\cdot - k)\}_{1\le j\le r, n, k\in\mathbb{Z}}. \tag{3.2}$$

will form a tight frame for $L_2(\mathbb{R})$, if the masks $\{h_0, h_1, \ldots, h_r\}$ satisfy

$$\sum_{j=0}^{r}\sum_{n\in\Omega_k} (h_j[n])^* h_j[n+m] = 2^{-1}\delta_{m,0} \tag{3.3}$$

for all $m \in \mathbb{Z}$, $k \in \mathbb{Z}/2\mathbb{Z}$, where $\Omega_k = (2\mathbb{Z} + k) \cap \operatorname{supp}(h_0)$. The set of masks $H = \{h_0, h_1, \ldots, h_r\}$ is often called *wavelet filter bank*.

For wavelet bi-frames, suppose that we have two refinable functions $\phi, \widetilde{\phi}$ with refinable masks $h_0, \widetilde{h}_0$, and each of which admits an MRA for $L_2(\mathbb{R})$. Define two sets of framelets $\Psi = \{\psi_j\}_{j=1}^r, \widetilde{\Psi} = \{\widetilde{\psi}_j\}_{j=1}^r$ as follows,

$$\psi_j(\cdot) = 2\sum_{k\in\mathbb{Z}} h_j[k]\phi(2\cdot - k); \quad \widetilde{\psi}_j(\cdot) = 2\sum_{k\in\mathbb{Z}} \widetilde{h}_j[k]\widetilde{\phi}(2\cdot - k),$$

for $j = 1, \ldots, r$. Then, the MEP [17] shows that under very mild conditions, two wavelet (affine) systems given by

$$X(\Psi) = \{2^{n/2}\psi_j(2^n\cdot - k)\}_{1\le j\le r; n, k\in\mathbb{Z}}; \quad X(\widetilde{\Psi}) = \{2^{n/2}\widetilde{\psi}_j(2^n\cdot - k)\}_{1\le j\le r; n, k\in\mathbb{Z}}.$$

form bi-frames for $L_2(\mathbb{R})$, if the two mask sets $\{h_j\}_{j=0}^r$ and $\{\widetilde{h}_j\}_{j=0}^r$ satisfy

$$\sum_{j=0}^{r}\sum_{n\in\Omega_k}(h_j[n])^*\widetilde{h}_j[n+m]=2^{-1}\delta_{m,0}. \tag{3.4}$$

In the context of signal processing, it is often more preferred to use a shift-invariant system. Recall that a system X is called shift-invariant if for any $g\in X$ and any $k\in\mathbb{Z}$, we have $g(\cdot-k)\in X$. To have such a shift-invariant property, the wavelet system $X(\Psi)$ needs to be over-sampled for the level $n<0$, which is called a quasi-affine system. More specifically, consider a wavelet system $X(\Psi)=\{2^{n/2}\psi_j(2^n\cdot-k)\}_{1\le j\le r;n,k\in\mathbb{Z}}$, its quasi-affine version from level 0, denoted by $X^q(\Psi)=\{\psi^q_{j,n,k}\}_{1\le j\le r,n,k\in\mathbb{Z}}$, is defined by

$$\psi^q_{j,n,k}=\begin{cases}2^{n/2}\psi_j(2^n\cdot-k), & n\ge 0,\\ 2^n\psi_j(2^n\cdot-2^nk), & n<0.\end{cases}$$

If $X(\Psi)$ is a tight wavelet frame for $L_2(\mathbb{R})$ obtained from the UEP, the quasi-affine system $X^q(\Psi)$ defined above also forms a tight frame for $L_2(\mathbb{R})$. More details regarding quasi-affine systems and tight frames can be found in [33].

3.2. Multi-level discrete framelet transform. Once an MRA-based wavelet bi-frames or tight frames for $L_2(\mathbb{R})$ are constructed via the construction of the masks satisfying the MEP or UEP, we have in hand a filter bank (the set of masks) based efficient numerical implementation of multi-level decomposition and reconstruction for discrete signals. For simplicity, we only present the discrete framelet transform with finite supported filter bank on the sequence space $\ell(\mathbb{Z})$, it can be easily generalized to the finite signal space $\mathbb{C}^N$ by periodic boundary extension. Discrete framelet transform has two parts: framelet decomposition and framelet reconstruction, and they are built on three basic operations. One is discrete convolution:

$$(f\otimes h)[m]=\sum_{k\in\mathrm{supp}(h)}h[k]f[m-k],\quad \text{for any } f\in\ell(\mathbb{Z}),$$

where h denotes a filter in $\ell_0(\mathbb{Z})$. One is down-sampling operator:

$$(f\downarrow_2)[k]=f[2k], \tag{3.5}$$

and the other is up-sampling operator:

$$(f\uparrow_2)[k]=\begin{cases}f[\frac{k}{2}], & \text{if } \frac{k}{2}\in\mathbb{Z},\\ 0, & \text{otherwise.}\end{cases} \tag{3.6}$$

There are two basic operators involved in framelet transform. Given a filter $h\in\ell_0(\mathbb{Z})$, one is the transit operator $W_h:\ell(\mathbb{Z})\to\ell(\mathbb{Z})$ defined by

$$W_hf=(f\otimes h^*[-\cdot])\downarrow_2. \tag{3.7}$$

The other is subdivision operator: $W_h^*:\ell(\mathbb{Z})\to\ell(\mathbb{Z})$ defined by

$$W_h^*c=(c\uparrow_2)\otimes h. \tag{3.8}$$

Let $H = \{h_0, h_1, \dots, h_r\} \subset \ell_0(\mathbb{Z})$ denote the filter bank that defines wavelet frame $X(\Psi)$, and $\widetilde{H} = \{\widetilde{h}_0, \widetilde{h}_1, \dots, \widetilde{h}_r\} \in \ell_0(\mathbb{Z})$ the filter bank that defines the dual frame $X(\widetilde{\Psi})$. In the case of wavelet tight frame, $H = \widetilde{H}$.

A one-level framelet transform comprises two operators: decomposition and reconstruction. The decomposition operator W_H: $\ell(\mathbb{Z}) \to \ell(\mathbb{Z})^{1\times(r+1)}$ is defined as: for any $f \in \ell(\mathbb{Z})$,

$$W_H f := (W_{h_0} f, W_{h_1} f, \dots, W_{h_r} f). \tag{3.9}$$

The reconstruction operator $W^*_{\widetilde{H}}$: $\ell(\mathbb{Z})^{1\times(r+1)} \to \ell(\mathbb{Z})$ is defined by:

$$W^*_{\widetilde{H}} c = W^*_{\widetilde{h}_0} c_0 + W^*_{\widetilde{h}_1} c_1 + \cdots + W^*_{\widetilde{h}_r} c_r. \tag{3.10}$$

Then, *perfect reconstruction property* of bi-frames or tight frames leads to

$$W^*_{\widetilde{H}} W_H = I \quad \text{(bi-frames)}, \quad \text{and} \quad W^*_H W_H = I \quad \text{(tight frames)},$$

where I is identity operator.

One motivation of discrete framelet transform is for effectively extracting multi-scale structures of input signals, which requires the so-called multi-level discrete framelet transform. Multi-level discrete framelet transform is done by recursively performing one-level discrete framelet transform on only one selected sequence of framelet coefficients, which is called low-pass framelet coefficients generated from a low-pass filter (the refinement mask h_0). The framelet coefficients and their associated filters in other sequences, which are not selected for further decomposition, are called high-pass framelet coefficients and high-pass filters (the wavelet masks $\{h_1, \dots, h_r\}$). Let W_h and W^*_h denote the transit operator and subdivision operator defined as (3.7) and (3.8) respectively. Then, the decomposition procedure of an L-level framelet transform reads as follows. Initialize $c_0^{(0)} = f$. For $\ell = 1, 2, \cdots, L$,

$$c_j^{(\ell)} = W_{h_j} c_0^{(\ell-1)}, \quad \text{for } j = 0, 1, \dots, r. \tag{3.11}$$

The coefficients $\{c_1^{(\ell)}, c_2^{(\ell)}, \dots, c_r^{(\ell)}\}_{\ell=1}^{L} \cup c_0^{(L)}$ are the L-level framelet coefficients of f. The reconstruction procedure reads as follows. For $\ell = L-1, \cdots, 1, 0$,

$$c_0^{(\ell)} = \sum_{j=0}^{r} W^*_{\widetilde{h}_j} c_j^{(\ell+1)}. \tag{3.12}$$

The signal f is then set as $f = c_0^{(0)}$. Recursively applying the perfect reconstruction property on each level, we also have the perfect reconstruction property for an L-level framelet transform. Interesting readers are referred to [15, 17, 42] for more details on MRA-based wavelet bi-frames, wavelet tight frames and discrete framelet transform.

The framelet transform introduced above is derived from the standard MRA-based wavelet tight frames or bi-frames for $L_2(\mathbb{R})$. For shift-invariant version of wavelet frames, we can define the so-called undecimal discrete framelet transform, which removes down-sampling operation in decomposition and up-sampling operation in reconstruction. Given a finite filter h, the transit operator W_h and the subdivision operator W^*_h are defined by

$$W_h f = f \otimes h^*(-\cdot), \quad \text{and} \quad W^*_h f = f \otimes h.$$

Recall that in decimal case, the coefficients at the coarser level have been down-sampled, while the coefficients at the coarser level in undecimal case have not been down-sampled. Notice that

$$(h \otimes (f \downarrow_{2^{\ell-1}})) = \big((h \uparrow_{2^{\ell-1}}) \otimes f\big) \downarrow_{2^{\ell-1}},$$

which says the undecimal version of a down-sampled signal $f \downarrow_{2^\ell-1}$ convolved with a filter h is indeed the original signal f convolved with the upsampled filter $h \uparrow_{2^\ell-1}$. Thus, at the ℓ-th level, the transit operator $W_h^{(\ell)}$ and subdivision operator $(W_h^*)^{(\ell)}$ are given by

$$W_h^{(\ell)} f = (h^{(\ell)})^*(-\cdot) \otimes f, \quad \text{and} \quad (W_h^*)^{(\ell)} f = h^{(\ell)} \otimes f.$$

where $h^{(\ell)} = h \uparrow_{2^{\ell-1}}$.

3.3. Basics on graph theory. Recall that a graph $G = (\mathcal{V}, E, \omega)$ comprises a set of vertices $\mathcal{V} = \{v_p : p = 1, ..., N\}$, a set of edges $E \subset \mathcal{V} \times \mathcal{V}$ and a weight function $\omega : E \to \mathbb{R}^+$. Its *adjacency matrix* S is an $N \times N$ matrix defined by

$$S[p,q] = \begin{cases} \omega(v_p, v_q), & (v_p, v_q) \in E, \\ 0, & \text{otherwise}, \end{cases} \quad \text{for } 1 \le p, q \le N.$$

The degree matrix, denoted by D, is a diagonal matrix with its k-th diagonal element given by $D[k,k] = \sum_{p=1}^N S[k,p]$.

In this paper, we only consider signals defined on an undirected connected graph, which satisfies the following properties:

- *Undirected*: $(v_p, v_q) \in E$ if and only if $(v_q, v_p) \in E$, and $\omega(v_p, v_q) = \omega(v_q, v_p)$ for any $v_p, v_q \in V$.
- *Connected*: there is a path between every pair of vertices in G.
- There exists no loop (an edge connecting a vertex to itself).

For a connected undirected graph, its adjacency matrix S satisfies the following properties:

1. The matrix S is symmetric.
2. The summation $\sum_{j=1}^{N-1} S^j$ has no zero entries.
3. All diagonal entries of S are zero.

Then, a signal $f = (f[1]; f[2]; \ldots; f[N])$, is a function defined on the vertices of the graph $G = (\mathcal{V}, E, \omega)$, i.e., $f : \quad \mathcal{V} \to \mathbb{C}^N$.

4. Key ingredients of discrete framelet transform on graph. Before presenting undecimal framelet transform for signals on undirected graph, we first present in this section the generalization of several basic concepts in signal processing, namely shift, convolution, down-sampling and up-sampling, from equispaced Euclidean grids to undirected graph. Consider a signal $f \in \mathbb{C}^N$ defined on the vertices of a graph $G = \{\mathcal{V}, E, \omega\}$. Let $S \in \mathbb{C}^{N \times N}$ denote the adjacency matrix of G, and let D denote its degree matrix. Then, the matrix

$$D^{-\frac{1}{2}} S D^{-\frac{1}{2}}$$

is called the normalized adjacency matrix whose eigenvalues are inside $[-1, 1]$ (see e.g. [8]). In the next, we define the shift operator for undirected graph, which defines how a signal is translated around the vertices of a graph. Such a shift operation is essential for defining discrete convolution.

DEFINITION 1 (Graph shift operator). *Consider an undirected graph G with adjacency matrix $S \in \mathbb{R}^{N\times N}$. A matrix $\mathcal{T} \in \mathbb{C}^{N\times N}$ is called the unit shift operator of G, if $\mathcal{T}$ is invertible, normal and satisfies*

$$D^{-\frac{1}{2}} S D^{-\frac{1}{2}} = \frac{1}{2}(\mathcal{T} + \mathcal{T}^*). \tag{4.1}$$

The proposed definition for the shift operator is different from existing definitions of shift operator on graphs, which usually directly treats S as the shift operator. In Definition 1, $\mathcal{T}$ is viewed as the shift operator by 1-tap and its transpose $\mathcal{T}^*$ is also a shift operator by 1 tap but toward the opposite direction. Thus, the normalized adjacency matrix of an undirected graph is viewed the average of shifting the graph by 1 tap on both directions. For any $k \in \mathbb{Z}$, the k-tap shift operator is defined as $\mathcal{T}^k$. The graph shift operator in Definition 1 keeps many desired properties of its counterpart for equispaced grids. To list some,

- The invertibility of $\mathcal{T}$ implies that shifting signal on graph will not remove information of signal.
- The property $\mathcal{T}^*\mathcal{T} = \mathcal{T}\mathcal{T}^*$ implies that shifting signals forward and shifting signal backward should be commutative.
- The fact $\mathcal{T}^{k_1}\mathcal{T}^{k_2} = \mathcal{T}^{k_1+k_2}$ implies that the shifts of the signal are accumulated.

By Definition 1, the shift operator is not unique. In the next, we present the construction scheme of a special type of shift operators, the isometric shift operator that preserves the energy of signals, i.e. $\mathcal{T}$ is a unitary operator with $\mathcal{T}^*\mathcal{T} = I$. Isometry property is one basic property of shift operator for equispaced grids, i.e., a signal energy is kept when being shifted around over the graph. Isometry property of shift operator is certainly a desired property for signal processing. If the shift operator is not isometric, after being shifted for many taps, the component of the signal with respect to the largest eigenvalue will dominate the output, and all others disappear. Such a behavior certainly causes computational instability and inconsistency for multi-level analysis which involves the concatenation of many convolutions.

CONSTRUCTION 1. *[Isometric shift operator] Let S denote the adjacency matrix of an undirected graph G. Then $D^{-\frac{1}{2}} S D^{-\frac{1}{2}}$ is symmetric, whose eigenvalues lie in $[-1, 1]$. Let $U \in \mathbb{C}^{N\times N}$ denote the unitary matrix that diagonalizes the matrix S:*

$$D^{-\frac{1}{2}} S D^{-\frac{1}{2}} = U^{-1}\Sigma U,$$

where $\Sigma = \mathrm{diag}(\underbrace{\mu[1], \ldots, \mu[1]}_{m_1}, \underbrace{\mu[2], \ldots, \mu[2]}_{m_2}, \ldots, \underbrace{\mu[p], \ldots, \mu[p]}_{m_p})$. *Define the shift operator $\mathcal{T}$ as*

$$\mathcal{T} = U^{-1}\Lambda U = U^{-1}\mathrm{diag}(\lambda[1], \lambda[2], \ldots, \lambda[N])U.$$

Then, the matrix $\mathcal{T}$ is unitary and satisfies (4.1), if we set

$$\lambda[k] = e^{i\theta_k}, \quad \textit{with} \quad \cos(\theta_k) = \mu[j_k], \tag{4.2}$$

where for the same $\mu[j_k]$, the value θ is assigned alternatively between $\theta_k \in [0, \pi)$ and $2\pi - \theta_k$. That is, for $j = 1, 2, \ldots, p$,

$$\lambda[(\sum_{n=1}^{j-1} m_n) + k] := \mu[j] + i(-1)^{k-1}\sqrt{1 - (\mu[j])^2}, \quad \textit{for} \quad k = 1, \ldots, m_j. \tag{4.3}$$

The shift operator constructed in Construction 1 essentially takes the eigenvectors of adjacent matrix as its eigenvectors and maps the eigenvalues of the adjacent matrix in $[-1, 1]$ to the unit disk in complex plane. Clearly, such a shift operator is unitary which preserves the energy when shifting the signal around the graph. Such an energy-preserving property is similar to its counterpart in classic equispaced grids, and does not attenuate any components of signals when being applied for multiple times. The trade-off is that in general it is not likely to have a sparse shift operator $\mathcal{T}$ even when the adjacency matrix S is sparse.

With the availability of graph shift operator $\mathcal{T}$, we now define convolution operator for a finite filter $h = \{h[k]\}_{k\in\mathbb{Z}_M}$. For simplicity, we restrict the filter size no larger than N.

Definition 2 (Graph convolution operator). *Consider a finite filter $h = \{h[k]\}_{k\in\mathbb{Z}_M}$ and a graph G. The convolution operator is defined as: for any signal $f \in \mathbb{C}^N$,*

$$\mathcal{H}(h)f = \sum_{k\in\mathbb{Z}_M} h[k]\mathcal{T}^k f, \tag{4.4}$$

where $\mathcal{T}$ denotes the shift operator defined in Definition 1.

By the basic property of matrix multiplication, we have

Proposition 4.1 (Shift-invariance of convolution operator). *Let $\mathcal{T}$ and $\mathcal{H}(h)$ denote the shift operator and the convolution operator w.r.t. the filter h. Then, for any signal $f \in \mathbb{C}^N$,*

$$\mathcal{H}(h)(\mathcal{T}^k f) = \mathcal{T}^k(\mathcal{H}(h)f).$$

In the next, we define another key block involved in framelet transform: dyadic down-sampling and up-sampling operators for signals on graph G. Motivated by basic properties of their counterparts for equispaced grids, we proposed the following generalized down/up sampling operator such that down-sampling an up-sampled signal does not lose the information of the signal.

Definition 3 (Dyadic down(up)-sampling operator on graph). *The operator $\Gamma_\downarrow \in \mathbb{C}^{\frac{N}{2}\times N}$ and its adjoint operator $\Gamma_\uparrow = (\Gamma_\downarrow)^*$ are called the down-sampling operator and up-sampling operator, provided that $\Gamma_\downarrow\Gamma_\uparrow \in \mathbb{C}^{\frac{N}{2}\times\frac{N}{2}}$ is invertible.*

Clearly, the definition of down/up-sampling is not unique. In the next, we give a construction scheme of down/up sampling operator satisfying the conditions imposed in Definition 3, which is analogy to the reconstruction property of classical down-sampling operator on bandlimited signal. More specifically, it is known that in 1D uniform grid, whether a signal can be perfectly reconstructed from is samples depends on whether its frequencies fall into the interval determined by Shannon sampling theorem. Thus, if a signal is bandlimited with the upper-half of its frequency spectrum vanishes, the signal still can be exactly recovered from samples after being down-sampled. Before introducing the down-sampling operator on graph that keeps such a property, we first introduce the generalization of discrete Fourier transform from equispaced grids to graphs.

The definition of discrete Fourier transform on graph is then based on one fundamental property of classic discrete Fourier transform, i.e., the classic discrete Fourier transform is the matrix that diagonalizes the shift operator or equivalently the finite convolution operator on equispaced grids. Recall that by Definition 1, $\mathcal{T}$ is an invertible normal matrix. Thus, there exists a unitary matrix V such that

$$\mathcal{T} = V^{-1}\Lambda V = V^{-1}\mathrm{diag}(\lambda[1], \ldots, \lambda[N])V$$

where $\{\lambda[k]\}_{k=1}^N$ are eigenvalues of $\mathcal{T}$, and they can be viewed as the generalized frequencies.

DEFINITION 4 (Discrete Fourier transform on graph (GDFT)). *For a graph G, its discrete Fourier transform on graph is the unitary matrix $\mathcal{F} \in \mathbb{C}^{N\times M}$ that diagonalizes the shift operator $\mathcal{T}$:*

$$\mathcal{F}\mathcal{T}\mathcal{F}^{-1} = \mathrm{diag}(\lambda[1], \lambda[2], \ldots, \lambda[N]).$$

It can be seen that when we adopt the shift operator defined in Construction 1, the GDFT $\mathcal{F}$ is the same as the unitary matrix that diagonalizes the adjacency matrix.

PROPOSITION 4.2 (Convolution theorem). *Let $\mathcal{H}$ and $\mathcal{F}$ denote the convolution operator and discrete Fourier transform defined in Definition 2 and 4 respectively. Then, $\mathcal{F}\mathcal{H}\mathcal{F}^{-1}$ is a diagonal matrix.*

Proof. By the definition $\mathcal{F}$ and $\mathcal{H}$, we have

$$\mathcal{H}(h) = \sum_{k\in\mathbb{Z}_M} h[k]\mathcal{T}^k = \sum_{k\in\mathbb{Z}_M} h[k]\big(\mathcal{F}^{-1}\Lambda\mathcal{F}\big)^k = \mathcal{F}^{-1}\big(\sum_{k\in\mathbb{Z}_M} h[k]\Lambda^k\big)\mathcal{F}.$$

Since $\sum_{k\in\mathbb{Z}_M} h[k]\Lambda^k$ is a diagonal matrix, we have $\mathcal{F}\mathcal{H}\mathcal{F}^{-1}$ is a diagonal matrix. ∎

Recall that up-sampling and down-sampling on equispaced grids, expressed in vertex domain as (3.5) and (3.6), can also be expressed in frequency domain in terms of frequency folding operation. Let $\widehat{\cdot}$ denote the classical discrete Fourier transform. Then, we have

$$\widehat{(f\downarrow_2)}[k] = \frac{1}{2}\left(\widehat{f}[k] + \widehat{f}[k+\frac{N}{2}]\right), \quad \text{for} \quad k = 1, \ldots, \frac{N}{2},$$

where $\widehat{f}[k]$ refers the frequency $e^{i2\pi\frac{k-1}{N}}$. In other words, down-sampling on equi-spaced grid is the same as folding its frequencies by one half. To generalize it from equispaced grid to graph, one first needs to assign the frequency magnitude to each eigenvalue of $\mathcal{T}$, so that the eigenvalues of $\mathcal{T}$ can be appropriately ordered to making meaningful frequency folding.

Motivated by graph total-variation based frequency analysis [39], the frequency associated with an eigenvalue $\lambda[k]$ is determined by the number of the oscillations of the corresponding eigenvectors $\mathcal{F}_k^{-1}$, which is measured by its generalized total variation:

$$\|\nabla\mathcal{F}_k^{-1}\|_1 = \|(I-\mathcal{T})F_k^{-1}\|_1 = |1-\lambda[k]|\cdot\|\mathcal{F}_k^{-1}\|_1.$$

Then, we consider the following ordering strategy of eigenvalues in terms of frequency magnitude, i.e.

$$\mathcal{F}\mathcal{T}\mathcal{F}^{-1} = \mathrm{diag}(\lambda[1], \lambda[2], \ldots, \lambda[N]),$$

such that the corresponding eigenvectors satisfy

$$\|\nabla\mathcal{F}_1^{-1}\|_1 \le \|\nabla\mathcal{F}_N^{-1}\|_1 \le \|\nabla\mathcal{F}_2^{-1}\|_1 \le \|\nabla\mathcal{F}_{N-1}^{-1}\|_1 \le \cdots \le \|\nabla\mathcal{F}_{\frac{N}{2}}^{-1}\|_1 \le \|\nabla\mathcal{F}_{\frac{N}{2}+1}^{-1}\|_1. \tag{4.5}$$

CONSTRUCTION 2. *[Bandlimited down/up-sampling operator] Let $\mathcal{F}$ denote the graph discrete Fourier transform, whose columns follow the order (4.5). Recall that $\mathcal{F}\in\mathbb{C}^{N\times N}$ is a unitary matrix. Thus the matrix $\big(I_{N/2}, I_{N/2}\big)\mathcal{F} \in \mathbb{C}^{\frac{N}{2}\times N}$ is of full row rank, and we form a matrix $\overline{V}\in\mathbb{C}^{\frac{N}{2}\times\frac{N}{2}}$ whose columns contains $N/2$ linearly independent columns of $\big(I_{N/2}, I_{N/2}\big)\mathcal{F}$. Consider the QR decomposition of $\overline{V}$:*

$$\overline{V} = \overline{U}R, \tag{4.6}$$

where $\overline{U} \in \mathbb{C}^{\frac{N}{2}\times\frac{N}{2}}$ *is a unitary matrix and* $R \in \mathbb{C}^{\frac{N}{2}\times\frac{N}{2}}$ *is an upper triangular matrix. Then, we define the down-sampling and up-sampling operators,* $\Gamma_\downarrow$ *and* $\Gamma_\uparrow$*, by*

$$\Gamma_\downarrow = \frac{1}{\sqrt{2}}\big(\overline{U}^*, \overline{U}^*\big)\mathcal{F} \quad \textit{and} \quad \Gamma_\uparrow = \frac{1}{\sqrt{2}}\mathcal{F}^* \begin{pmatrix} \overline{U} \\ \overline{U} \end{pmatrix}. \tag{4.7}$$

Indeed, the down/up-sampling operator constructed in Construction 2 satisfies the condition imposed in Definition 3 by the fact that

$$\Gamma_\downarrow\Gamma_\uparrow = \frac{1}{2}\big(\overline{U}^*, \overline{U}^*\big)\mathcal{F}\mathcal{F}^* \begin{pmatrix} \overline{U} \\ \overline{U} \end{pmatrix} = \frac{1}{2}(\overline{U}^*U + \overline{U}^*U) = I_{N/2}.$$

Proposition 4.3. *Let* $\Gamma_\downarrow$ *and* $\Gamma_\uparrow$ *be the down-sampling and up-sampling operators defined in Construction 2. Then* $\Gamma_\downarrow^* = \Gamma_\uparrow$ *and* $\Gamma_\downarrow\Gamma_\uparrow$ *is invertible.*

A signal $f \in \mathbb{C}^N$ defined on the graph G is called band-limited if its frequencies vanish outside the half of the frequency domain:

$$(\mathcal{F}f)[k] = 0, \quad \text{for } \frac{N}{2} - \lfloor\frac{N}{4}\rfloor + 1 \le k \le \frac{N}{2} + \lceil\frac{N}{4}\rceil. \tag{4.8}$$

Proposition 4.4 (Band-limited down-sampling). *Consider a band-limited signal* $f \in \mathbb{C}^N$ *satisfying* (4.8) *with even-length. Let* $\Gamma_\downarrow$ *denote the down-sampling operator defined by* (4.7)*. Then, f can be perfectly reconstructed from* $\Gamma_\downarrow f$*.*

Proof. Consider a band-limited signal $f \in \mathbb{C}^N$ satisfying (4.8). Note that

$$\Gamma_\downarrow f = \frac{1}{\sqrt{2}}\overline{U}^*\big(I, I\big)\mathcal{F}f = \frac{1}{\sqrt{2}}\overline{U}^* \begin{pmatrix} (\mathcal{F}f)[1] \\ (\mathcal{F}f)[2] \\ \vdots \\ (\mathcal{F}f)[\frac{N}{2} - \lfloor\frac{N}{4}\rfloor] \\ (\mathcal{F}f)[\frac{N}{2} + \lceil\frac{N}{4}\rceil + 1] \\ \vdots \\ (\mathcal{F}f)[N-1] \\ (\mathcal{F}f)[N] \end{pmatrix}.$$

Then $f = \mathcal{F}^*\mathcal{F}f = \mathcal{F}^*x$, where $x \in \mathbb{C}^N$ is defined as

$$x[n] = \begin{cases} \sqrt{2}(\overline{U}\Gamma_\downarrow f)[n] & 1 \le n \le \frac{N}{2} - \lfloor\frac{N}{4}\rfloor \\ 0 & \frac{N}{2} - \lfloor\frac{N}{4}\rfloor + 1 \le n \le \frac{N}{2} + \lceil\frac{N}{4}\rceil \\ \sqrt{2}(\overline{U}\Gamma_\downarrow f)[n - \frac{N}{2}] & \frac{N}{2} + \lceil\frac{N}{4}\rceil + 1 \le n \le N \end{cases}.$$

Therefore, f can be perfectly reconstructed from $\Gamma_\downarrow f$. ∎

Example 1. *The basic operations introduced for signals on graph in this section are consistent with their counterparts for signals on 1D equispaced Euclidean grid with periodic boundary extension. Consider a finite signal* $f \in \mathbb{C}^N$ *with periodic boundary extension. Then, the corresponding*

Algorithm 4.1 Key procedures of framelet transform on graph

- **Isometric shift operator**: $\mathcal{T}$
  1: Compute the eigenvalue decomposition of normalized adjacency matrix:
  $$D^{-\frac{1}{2}} S D^{-\frac{1}{2}} = U^{-1} \Sigma U$$
  2: Set $\Lambda = \mathrm{diag}(\lambda[1], \lambda[2], \ldots, \lambda[N])$, where $\lambda[k]$ $(1 \le k \le N)$ is computed by (4.3)
  3: Set $\mathcal{T} = U^{-1} \Lambda U$
- **Graph discrete Fourier transform**: $\mathcal{F}$
  1: Set $\mathcal{F} = U$
- **Graph convolution operator**: $\mathcal{H}$
  1: Set $\mathcal{H}(h) = \sum_{k \in \mathbb{Z}_M} h[k] \mathcal{T}^k$
- **Down(up)-sampling operator**: $\Gamma_\downarrow (\Gamma_\uparrow)$
  1: Define $\overline{V}$ by extracting $N/2$ linearly independent columns of $\left(I_{N/2}, I_{N/2}\right) \mathcal{F}$
  2: Compute the QR decomposition of $\overline{V}$: $\overline{V} = \overline{U} R$
  3: Set
  $$\Gamma_\downarrow = \frac{1}{\sqrt{2}} \left(\overline{U}^*, \overline{U}^*\right) \mathcal{F} \quad \text{and} \quad \Gamma_\uparrow = \frac{1}{\sqrt{2}} \mathcal{F}^* \begin{pmatrix} \overline{U} \\ \overline{U} \end{pmatrix}$$

adjacency matrix is given by

$$S = \begin{pmatrix} 0 & 1 & & & 1 \\ 1 & 0 & 1 & & \\ & 1 & 0 & & \\ & & & \ddots & 1 \\ 1 & & & 1 & 0 \end{pmatrix}.$$

Then the classic discrete Fourier transform $\mathcal{F}$ defined by

$$\mathcal{F}[j,k] = N^{-\frac{1}{2}} e^{\mathrm{i}2\pi \frac{(j-1)(k-1)}{N}}, \quad 1 \le j,k \le N.$$

will diagonalize the matrix S:

$$\mathcal{F}^{-1} S \mathcal{F} = 2 \cdot \mathrm{diag}(1, \cos\frac{2\pi}{N}, \cos\frac{4\pi}{N}, \ldots, \cos\frac{2(N-1)\pi}{N}).$$

By the construction scheme proposed in Construction 1 for the graph shift operator $\mathcal{T}$, we have

$$\mathcal{T} = \mathcal{F}^{-1} \left(\mathrm{diag}(1, e^{\frac{\mathrm{i}2\pi}{N}}, e^{\frac{\mathrm{i}2\pi 2}{N}}, \ldots, e^{\frac{\mathrm{i}2\pi(N-1)}{N}})\right) \mathcal{F},$$

whose matrix form is

$$\begin{pmatrix} 0 & & & 1 \\ 1 & 0 & & \\ & & \ddots & \\ & & 1 & 0 \end{pmatrix}.$$

Thus, $\mathcal{T}^k$ is exactly the k-tap shift operator:

$$\mathcal{T}^k : f[n] \to f[(n-k) \bmod N],$$

and the discrete convolution defined in Definition 2 is also the same as classic discrete convolution with periodic boundary extension:

$$(f \otimes h)[n] = \sum_{k \in \mathrm{supp}(h)} h[k] f[(n-k) \bmod N].$$

For dyadic down-sampling operator, we have

$$\Gamma_\downarrow = \begin{pmatrix} 1 & 0 & 0 & \cdots & 0 & 0 & 0 \\ 0 & 0 & 1 & \cdots & 0 & 0 & 0 \\ & & & \ddots & & & \\ 0 & 0 & 0 & \cdots & 1 & 0 & 0 \\ 0 & 0 & 0 & \cdots & 0 & 0 & 1 \end{pmatrix} \in \mathbb{C}^{\frac{N}{2} \times N} \tag{4.9}$$

and $\Gamma_\uparrow = (\Gamma_\downarrow)^*$. It is also consistent with classic dyadic down-sampling and up-sampling operator for signals on equispaced grids.

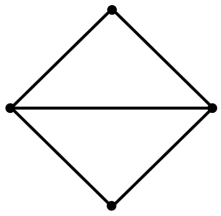

FIG. 4.1. *Diamond graph*

EXAMPLE 2. *Consider the diamond graph G with 5 nodes and 5 edges as shown in Figure 4.1. The adjacency matrix is given by*

$$S = \begin{pmatrix} 0 & 1 & 1 & 1 \\ 1 & 0 & 1 & 0 \\ 1 & 1 & 0 & 1 \\ 1 & 0 & 1 & 0 \end{pmatrix}.$$

Then by Algorithm 4.1, the discrete Fourier transform of G can be defined as

$$\mathcal{F} = \frac{1}{\sqrt{10}} \begin{pmatrix} \sqrt{3} & \sqrt{2} & \sqrt{3} & \sqrt{2} \\ \sqrt{5} & 0 & -\sqrt{5} & 0 \\ -\sqrt{2} & +\sqrt{3} & -\sqrt{2} & \sqrt{3} \\ 0 & -\sqrt{5} & 0 & \sqrt{5} \end{pmatrix},$$

which diagonalizes the normalized adjacency matrix

$$D^{-\frac{1}{2}} S D^{-\frac{1}{2}} = \mathcal{F}^{-1} \mathrm{diag}(1, -\frac{1}{3}, -\frac{2}{3}, 0) \mathcal{F}.$$

According to Construction 1, the graph shift operator $\mathcal{T}$ is given by

$$\mathcal{T} = \mathcal{F}^{-1}\mathrm{diag}(1, -\frac{1}{3} + i\frac{2\sqrt{2}}{3}, -\frac{2}{3} + i\frac{\sqrt{5}}{3}, i)\mathcal{F}.$$

Consequently, the convolution operator with filter $h = \{h[k]\}_{k\in\mathbb{Z}_M}$ can be written as

$$\mathcal{H}(h) = \sum_{k\in\mathbb{Z}_M} h[k]\mathcal{T}^k.$$

For the down/up-sampling operator,

$$\Gamma_\downarrow = \frac{1}{\sqrt{50+10\sqrt{6}}}\begin{pmatrix} 2 & -5-\sqrt{6} & -3 & -\sqrt{6} \\ \sqrt{15} & 0 & -\sqrt{10} & \sqrt{10}+\sqrt{15}\end{pmatrix} \quad \textit{and} \quad \Gamma_\uparrow = (\Gamma_\downarrow)^*.$$

Example 3. *The basic operations defined in this section cannot directly replicate their counterparts for multi-dimensional signals (e.g. images and videos) defined on equispaced Euclidean grids with periodic boundary extension in $\mathbb{R}^d$. Nevertheless, as a d-dimensional equispaced Euclidean grid can be decomposed as the Cartesian product of d 1D equispaced Euclidean grids in $\mathbb{R}$, one can generalize the operations defined in this section to the graph which can factorized as the Cartisian product of 2 prime graphs.*

Briefly, consider a simple connected graph $G = \{\mathcal{V}, E, \omega\}$, which can be factorized as the Cartesian product of d prime graphs $G_q = \{\mathcal{V}_q, E_q, \omega_q\}$ $(1 \le q \le d)$, with $|\mathcal{V}_q| = N_q$ and $N = |\mathcal{V}| = \prod_{q=1}^d N_q$. In this case, the adjacency matrix of G can be written as

$$S = \sum_{q=1}^d \underbrace{I_{N_1}\otimes\ldots\otimes I_{N_{q-1}}}\otimes S_q \otimes \underbrace{I_{N_{q+1}}\otimes\ldots\otimes I_{N_d}} = \sum_{q=1}^d I_{\prod_{k=1}^{q-1}N_k}\otimes S_q \otimes I_{\prod_{k=q+1}^{d}N_k},$$

where $\otimes$ denotes the kronecker product, and S_q is the adjacency matrix of G_q.

Then the key operations for defining discrete framelet transform on such a graph G can be derived from the Kronecker product of the operations on each prime factor G_q, defined in the previus discussion. Given a d-tuple $\mathbf{k} = (k_1, \ldots, k_d) \in \mathbb{Z}^d$, the $\mathbf{k}$-shift operator $T(\mathbf{k})$ is defined by

$$T(\mathbf{k}) = \bigotimes_{q=1}^d \mathcal{T}_q^{k_q}, \tag{4.10}$$

where $\mathcal{T}_q$ denotes the shift operator on the prime graph G_q, as defined in Construction 1. Then, for a d-dimensional filter $h : \mathbb{Z}_M^d \to \mathbb{C}$, its associated convolution operator is given by

$$\mathcal{H}(h) = \sum_{\mathbf{k}\in\mathbb{Z}_M^d} h[\mathbf{k}]T(\mathbf{k}), \tag{4.11}$$

Similarly, the down-sampling and up-sampling operator on G is defined by

$$\Gamma_\downarrow = \bigotimes_{q=1}^d \Gamma_{\downarrow,q}; \quad \Gamma_\uparrow = \bigotimes_{q=1}^d \Gamma_{\uparrow,q}, \tag{4.12}$$

where $\Gamma_{\downarrow,q}, \Gamma_{\uparrow,q}$ denote the down-sampling and up-sampling operators of the prime graph G_q as defined in Construction 2.

5. Multi-level framelet transform on graph. After introducing the key building blocks for framelet transform on graph, we are ready to introduce multi-level framelet transform for signals on graph. Consider a signal $f \in \mathbb{C}^N$ defined on a connected undirected graph $G = \{\mathcal{V}, E, \omega\}$ with adjacency matrix S. Let $H = \{h_0, h_1, \ldots, h_r\}$ and $\widetilde{H} = \{\widetilde{h}_0, \widetilde{h}_1, \ldots, \widetilde{h}_r\}$ denote the filter banks for framelet decomposition and reconstruction respectively. In parallel to framelet transform on equispaced grids, the undecimal framelet transform on graph is also built on decimal framelet transform by removing down-sampling operator at each level.

For a finite filter h, the transit operator W_h^d and the subdivision operator $(W_h^d)^*$ are defined as

$$W_h^d = \Gamma_\downarrow \mathcal{H}(h^*(-\cdot)), \quad \text{and} \quad (W_h^d)^* = \mathcal{H}(h)\Gamma_\uparrow,$$

where the convolution matrix $\mathcal{H}(h)$ and down/up-sampling operators are defined as Definition 2 and Definition 3. Then, the one-level decimal framelet transform is given by

$$f \longrightarrow c := (W_{h_0}^d f; W_{h_1}^d f; \ldots; W_{h_r}^d f) \quad \text{(decomoposition)}, \tag{5.1}$$

and

$$c \longrightarrow (W_{\widetilde{h}_0}^d)^* c_0 + (W_{\widetilde{h}_1}^d)^* c_1 + \cdots + (W_{\widetilde{h}_r}^d)^* c_r \quad \text{(reconstruction)}. \tag{5.2}$$

It can be seen from that the one-level framelet transform depends on the shift operator $\mathcal{T}$ derived from the underlying graph. The L-level framelet transform for signals on graph G has the same recursive scheme as the counterpart for equispaced Euclidean grids, i.e., the one-level discrete framelet transform is recursively applied on the output generated by a low-pass filter to generate a multi-level decomposition of input signal. The main difference between equi-spaced grid and general graph lies in the changes of the underlying structure after down-sampling. The underlying graph remains an equispaced grid after down-sampling the signal on a equispaced grid. Thus, the shift operator keep the same across different levels, up to grid size. In contrast, for a general graph, a meaningful down-sampling operator with good abstraction will change the underlying graph structure of downsampled signals. In other words, the shift operator varies at different levels, which leads to different one-level framelet transform at different level.

In the next, we propose a recursive scheme for defining the shift operators at different levels:

$$\mathcal{T}^{(1)}, \mathcal{T}^{(2)}, \ldots, \mathcal{T}^{(L)},$$

for an undirected graph G.

Construction 3. *Let $\mathcal{T}^{(1)} = \mathcal{T}$ be the graph shift operator at the finest level given in Definition 1, which is derived from the normalized adjacency matrix of the graph. Let $\Gamma_\downarrow^{(1)}$/ $\Gamma_\uparrow^{(1)}$ be the bandlimited down/up-sampling operator defined in Construction 2. The construction of the graph shift operator $\mathcal{T}^{(2)}$ is then motivated by the observation on equispaced grids that shifting a down-sampled signal by 1-tap is closely related to down-sampling the original signal shifted by 2-tap. Notice that the band-limited down/up-sampling operator in Construction 2 has*

$$\Gamma_\downarrow \left((\mathcal{T})^2 + (\mathcal{T}^*)^2 \right) \Gamma_\uparrow = \overline{U}^* \widetilde{\Sigma} \overline{U}, \tag{5.3}$$

where $\overline{U} \in \mathbb{C}^{\frac{N}{2} \times \frac{N}{2}}$ is the unitary matrix defined from (4.6) and $\widetilde{\Sigma} \in \mathbb{C}^{\frac{N}{2} \times \frac{N}{2}}$ is a real-valued diagonal matrix. The shift operator $\mathcal{T}^{(2)} \in \mathbb{C}^{\frac{N}{2} \times \frac{N}{2}}$ for the second level is then defined as a normal and invertible matrix that satisfies

$$\mathcal{T}^{(2)} + \left(\mathcal{T}^{(2)} \right)^* = \overline{U}^* \widetilde{\Sigma} \overline{U}, \tag{5.4}$$

Since $\overline{U}^*\widetilde{\Sigma}\overline{U}$ is a Hermitian matrix, one can use Construction 1 to construct an isometric shift operator $\mathcal{T}^{(2)}$. The unitary matrix, denoted by $\mathcal{F}^{(2)} \in \mathbb{C}^{\frac{N}{2}\times\frac{N}{2}}$, that diagonalizes $\mathcal{T}^{(2)}$ is defined as the Fourier transform at the second level. For example, $\mathcal{F}^{(2)} = \overline{U}$ when $\mathcal{T}^{(2)}$ is the defining isometric shift operator in Construction 1. By the same procedure, one can recursively define $\mathcal{T}^{(3)}, \mathcal{T}^{(4)}, \ldots, \mathcal{T}^{(L)}$. By (5.3) and (5.4), we have

$$\mathcal{T}^{(\ell+1)} + (\mathcal{T}^{(\ell+1)})^* = \Gamma_{\downarrow}^{(\ell)} \left(\left(\mathcal{T}^{(\ell)}\right)^2 + \left((\mathcal{T}^{(\ell)})^*\right)^2 \right) \Gamma_{\uparrow}^{(\ell)}, \quad \ell = 1, \ldots, L-1. \tag{5.5}$$

It can be seen from the equation above that, shifting the signal by 1 tap in the coarser level is the same as shifting the signal by 2 taps in the finer level, in which two levels are related via down-sampling and up-sampling operations.

After defining the sequence of graph shift operators, for any filter h, we then have the definition of the convolution at the ℓ-th level:

$$H^{(\ell)}(h) = \sum_{k\in\mathrm{supp}(h)} h[k](\mathcal{T}^{(\ell)}))^k.$$

Now, we have the following recursive procedure for an L-level decimal framelet transform on graph:

$$\begin{array}{ll} \text{Decomposition}: & c_0^{(0)} := f, \quad c_j^{(\ell)} := W_{h_j}^{(\ell)} c_0^{(\ell-1)} \text{ for } 0 \le j \le r, 1 \le \ell \le L; \\ \text{Reconstruction}: & c_0^{(\ell)} := \sum_{j=0}^r (W_{\widetilde{h}_j}^*)^{(\ell+1)} c_j^{(\ell+1)} \text{ for } \ell = L-1, \ldots, 1, 0, \quad g := c_0^{(0)}, \end{array} \tag{5.6}$$

where

$$W_h^{(\ell)} = \Gamma_{\downarrow}^{(\ell)} H^{(\ell)}(h^*(-\cdot)), \quad \text{and} \quad (W_{\widetilde{h}}^*)^{(\ell)} = H^{(\ell)}(h)\Gamma_{\uparrow}^{(\ell)}.$$

In contrast to equispaced grids, for general graphs, it is very difficult to have a filter bank with small support, which can admit a decimal framelet transform with perfect reconstruction property. Taking a single-level decimal framelet transform for example.

PROPOSITION 5.1. *Let $H = \{h_j\}_{j=0}^r$ and $\widetilde{H} = \{\widetilde{h}_j\}_{j=0}^r$ be two sets of finite sequences supported inside $\mathbb{Z}_M$. Then, the single-level discrete framelet transform defined by (5.6) with $L = 1$ satisfies the perfect reconstruction property if and only if H and $\widetilde{H}$ satisfy the following conditions:*

$$\begin{cases} \sum_{j=0}^r \sum_{k\in\mathbb{Z}_M} \sum_{p\in\mathbb{Z}_M+k} \widetilde{h}_j[k] h_j^*[k-p]\lambda^p[m] = 2 \\ \sum_{j=0}^r \sum_{k\in\mathbb{Z}_M} \sum_{p\in\mathbb{Z}_M+k} \widetilde{h}_j[k] h_j^*[k-p]\lambda_\ell^k[m]\lambda^{p-k}[(m+\frac{N}{2}) \bmod N] = 0, \end{cases} \quad \text{for } 1 \le m \le N. \tag{5.7}$$

Proof. The one-level framelet transform defined in (5.6) has perfect reconstruction property if and only if

$$\sum_{j=0}^r W_{\widetilde{h}_j}^* W_{h_j} = I_N.$$

Notice that

$$\begin{aligned}\sum_{j=0}^{r} W_{\widetilde{h}_j}^* W_{h_j} &= \sum_{j=0}^{r} H(\widetilde{h}_j)\Gamma_\uparrow\Gamma_\downarrow H(h_j^*(-\cdot)) \\ &= \frac{1}{2}\sum_{j=0}^{r} H(\widetilde{h}_j)\mathcal{F}^{-1}\begin{pmatrix} I_{\frac{N}{2}} & I_{\frac{N}{2}} \\ I_{\frac{N}{2}} & I_{\frac{N}{2}} \end{pmatrix}\mathcal{F}\mathcal{H}(h_j^*(-\cdot)) \\ &= \frac{1}{2}\mathcal{F}^{-1}\left(\sum_{j=0}^{r}\sum_{k\in\mathbb{Z}_M}\sum_{p\in\mathbb{Z}_M+k}\widetilde{h}_j[k]h_j^*[k-p]\Lambda^k\begin{pmatrix} I_{\frac{N}{2}} & I_{\frac{N}{2}} \\ I_{\frac{N}{2}} & I_{\frac{N}{2}} \end{pmatrix}\Lambda^{p-k}\right)\mathcal{F}.\end{aligned}$$

Therefore, the perfect reconstruction property holds if and only if

$$\sum_{j=0}^{r}\sum_{k\in\mathbb{Z}_M}\sum_{p\in\mathbb{Z}_M+k}\widetilde{h}_j[k]h_j^*[k-p]\Lambda^k\begin{pmatrix} I_{\frac{N}{2}} & I_{\frac{N}{2}} \\ I_{\frac{N}{2}} & I_{\frac{N}{2}} \end{pmatrix}\Lambda^{p-k} = 2I_N,$$

which is equivalent to the following conditions, i.e. for any $1 \le m \le N$,

$$\begin{aligned}&\sum_{j=0}^{r}\sum_{k\in\mathbb{Z}_M}\sum_{p\in\mathbb{Z}_M+k}\widetilde{h}_j[k]h_j^*[k-p]\lambda^p[m] = 2,\\ &\sum_{j=0}^{r}\sum_{k\in\mathbb{Z}_M}\sum_{p\in\mathbb{Z}_M+k}\widetilde{h}_j[k]h_j^*[k-p]\lambda^k[m]\lambda^{p-k}[(m+\frac{N}{2}) \bmod N] = 0.\end{aligned}$$

This completes the proof. ∎

It can be seen that in order to guarantee the perfect reconstruction property of a one-level framelet transform on a general graph, the two filter banks H and $\widetilde{H}$ need to satisfy totally N bi-linear equations. As N is the number of vertices, the construction of such filter banks becomes increasingly difficult for the graph with large size.

REMARK 1. *When the graph is bi-partite whose spectrum is symmetric about the zero, e.g. cycle graph with an even number of vertices, the condition (5.7) can be simplified to*

$$\begin{aligned}&\textstyle\sum_{j=0}^{r}\sum_{k\in\mathbb{Z}_M}\sum_{p\in\mathbb{Z}_M+k}\widetilde{h}_j[k]h_j^*[k-p]\lambda^p[m] = 2,\\ &\textstyle\sum_{j=0}^{r}\sum_{k\in\mathbb{Z}_M}\sum_{p\in\mathbb{Z}_M+k}\widetilde{h}_j[k]h_j^*[k-p](-1)^{k-p}\lambda^p[m] = 0,\end{aligned} \tag{5.8}$$

which is exactly the UEP condition for classic framelet transform with perfect reconstruction property.

In the next, we present the undecimal discrete framelet transform which removes the down-sampling operation at each level. In parallel to the case of equispaced grid, the question is then what is the undecimal version of a down-sampled signal convolved with a filter, which is answered in the following proposition.

PROPOSITION 5.2. *Let the operators $\{\mathcal{T}^{(1)}, \mathcal{T}^{(2)}, \dots, \mathcal{T}^{(L)}\}$ denote the shift operators defined in Construction 3, which calls the construction schemes for shift operator and band-limited down/up sampling operator in Construction 1 and Construction 2. Let $(\mathcal{T}^{(\ell)}, \Gamma_\downarrow^{(\ell)}, \Gamma_\uparrow^{(\ell)})$ denote the shift*

operator and down/up sampling operator for the ℓ-th level. Then, there exists an invertible and normal matrix $\mathcal{T}_u^{(\ell+1)} \in \mathbb{C}^{N\times N}$ such that

$$\left(\mathcal{T}^{(\ell+1)}\right)^k \prod_{k=\ell}^{1} \Gamma_\downarrow^{(k)} = \prod_{k=\ell}^{1} \Gamma_\downarrow^{(k)} \left(\mathcal{T}_u^{(\ell+1)}\right)^k,$$

for any $k \in \mathbb{Z}$.

Proof. For the second level, let $\mathcal{T}^{(2)}$ denote the shift operator defined via Construction 3. Let $\Lambda^{(2)}$ denote the diagonal matrix associated with the eigenvalue decomposition of $\mathcal{T}^{(2)}$, i.e. $\mathcal{T}^{(2)} = \overline{U}^* \Lambda^{(2)} \overline{U}$. Then $\Lambda^{(2)}$ is invertible by the definition of $\mathcal{T}^{(2)}$. Define

$$\mathcal{T}_u^{(2)} = (\mathcal{F}^{(1)})^* \begin{pmatrix} \Lambda^{(2)} & \\ & \Lambda^{(2)} \end{pmatrix} \mathcal{F}^{(1)}, \tag{5.9}$$

where $\mathcal{F}^{(1)}$ denotes graph Fourier transform of the previous level. Then, we have for any $k \in \mathbb{Z}$,

$$\left(\mathcal{T}^{(2)}\right)^k \Gamma_\downarrow = \frac{1}{\sqrt{2}} \overline{U}^* \left(\Lambda^{(2)}\right)^k (I, I) \mathcal{F}^{(1)} = \Gamma_\downarrow \left(\mathcal{T}_u^{(2)}\right)^k.$$

Recursively applying the argument above, we have that

$$\left(\mathcal{T}^{(\ell+1)}\right)^k \prod_{k=\ell}^{1} \Gamma_\downarrow^{(k)} = \prod_{k=\ell}^{1} \Gamma_\downarrow^{(k)} \left(\mathcal{T}_u^{(\ell+1)}\right)^k, \quad k \in \mathbb{Z}$$

for $\ell = 1, 2, \ldots, L-1$. ∎

It can be seen from the proposition above that the undecimal version of the shift operator $\mathcal{T}^{(\ell)}$ at the ℓ-th level is the shift operator denoted by $\mathcal{T}_u^{(\ell)}$, where $\mathcal{T}_u^{(1)} = \mathcal{T}^{(1)}$, and for $\ell \geq 2$, $\mathcal{T}_u^{(\ell)}$ can be recursively defined by the formula (5.9). Therefore, the convolution on a down-sampled signal can be expressed as down-sampling a signal after another convolution:

$$\mathcal{H}^{(\ell)}(h)\Gamma_\downarrow^{(\ell-1)} = \Gamma_\downarrow^{(\ell-1)} \mathcal{H}_u^{(\ell)}(h),$$

where the new convolution $\mathcal{H}_u^{(\ell)}(h)$ is defined as

$$H_u^{(\ell)}(h) = \sum_{k\in \mathrm{supp}(h)} h[k](\mathcal{T}_u^{(\ell)}))^k.$$

Then, at the ℓ-th level, the transit operator and the subdivision operator in the undecimal case is defined by

$$W_h^{(\ell)} : f \to \mathcal{H}_u^{(\ell)}(h(-\cdot)^*)f, \quad \text{and} \quad (W_h^*)^{(\ell)} : f \to \mathcal{H}_u^{(\ell)}(h)f.$$

Now, all operations involved in the framelet transform at the ℓ-level are defined. For simplicity of discussion, we assume that N can be divided by 2^L for some positive integer L. See Algorithm 5.1 for the outline of the proposed recursive scheme of constructing shift, down(up)-sampling and convolution operators for decimal and undecimal framelet transform.

See Algorithm 5.2 for the outline of the undecimal framelet transform for signals on graph.

Algorithm 5.1 Recursive reconstruction scheme of basic operators of multi-level (un)decimal framelet transform

Input: filter h, $\mathcal{F}^{(1)}$, $\mathcal{T}^{(\ell)} = \left(\mathcal{F}^{(\ell)}\right)^* \Lambda^{(\ell)} \mathcal{F}^{(\ell)}$, and $\Gamma_{\downarrow}^{(\ell)} = \frac{1}{\sqrt{2}} \left(\left(\overline{U}^{(\ell)}\right)^*, \left(\overline{U}^{(\ell)}\right)^* \right) \mathcal{F}^{(\ell)}$

Output: The operators at the $(\ell+1)$-th level:

- **Fourier transform** $\mathcal{F}^{(\ell+1)}$:
$$\mathcal{F}^{(\ell+1)} = \overline{U}^{(\ell)}.$$
- **Shift operator** $\mathcal{T}^{(\ell+1)}$ $(\mathcal{T}_u^{(\ell+1)})$:
$$\begin{cases} \text{Decimal:} & \mathcal{T}^{(\ell+1)} + (\mathcal{T}^{(\ell+1)})^* = \Gamma_{\downarrow}^{(\ell)} \left(\left(\mathcal{T}^{(\ell)}\right)^2 + \left((\mathcal{T}^{(\ell)})^*\right)^2 \right) \Gamma_{\uparrow}^{(\ell)} \\ \text{Undecimal:} & \mathcal{T}_u^{(\ell+1)} = \left(F^{(1)}\right)^* \operatorname{diag}\big(\underbrace{\Lambda^{(\ell+1)}, \cdots, \Lambda^{(\ell+1)}}_{2^\ell} \big) F^{(1)} \end{cases}$$
where $\Lambda^{(\ell+1)}$ is the eigenvalue matrix of $\mathcal{T}^{(\ell+1)}$
- **Convolution operator** $H^{(\ell)}$ $(H_u^{(\ell)})$:
$$\begin{cases} \text{Decimal:} & H^{(\ell)}(h) = \sum_{k \in \operatorname{supp}(h)} h[k] (\mathcal{T}^{(\ell)}))^k; \\ \text{Undecimal:} & H_u^{(\ell)}(h) = \sum_{k \in \operatorname{supp}(h)} h[k] (\mathcal{T}_u^{(\ell)}))^k. \end{cases}$$
- **Down(up)-sampling operator**: $\Gamma_{\downarrow}^{(\ell+1)} (\Gamma_{\uparrow}^{(\ell+1)})$
  1: Define $\overline{V}^{(\ell+1)}$ by extracting $\frac{N}{2^{\ell+1}}$ linearly independent columns of $\left(I_{\frac{N}{2^{\ell+1}}}, I_{\frac{N}{2^{\ell+1}}} \right) \mathcal{F}^{(\ell+1)}$
  2: Compute the QR decomposition of $\overline{V}^{(\ell+1)}$: $\overline{V}^{(\ell+1)} = \overline{U}^{(\ell+1)} R^{(\ell+1)}$
  3: Set
$$\Gamma_{\downarrow}^{(\ell+1)} = \frac{1}{\sqrt{2}} \left(\left(\overline{U}^{(\ell+1)}\right)^*, \left(\overline{U}^{(\ell+1)}\right)^* \right) \mathcal{F}^{(\ell+1)} \quad \text{and} \quad \Gamma_{\uparrow}^{(\ell+1)} = \left(\Gamma_{\downarrow}^{(\ell+1)}\right)^*$$

In the next, we establish a sufficient condition on the two filter banks, $H = \{h_0, h_1, \ldots, h_r\}$ and $\widetilde{H} = \{\widetilde{h}_0, \widetilde{h}_1, \ldots, \widetilde{h}_r\}$, that admits the perfect reconstruction property of multi-level undecimal discrete framelet transform. Recall that the perfect reconstruction property refers to that the signal can be exactly recovered using frame reconstruction operator from its framelet decomposition coefficients. The perfect reconstruction property of L-level discrete framelet transform will hold true, as long as the one-level discrete framelet transform at each level has perfect reconstruction property, i.e.

$$(W_{\widetilde{H}}^*)^{(\ell)} W_H^{(\ell)} = \sum_{j=0}^{r} (W_{\widetilde{h}_j}^*)^{(\ell)} W_{h_j}^{(\ell)} = I_N, \tag{5.10}$$

for $\ell = 1, 2, \ldots, L$.

THEOREM 5.3 (Perfect reconstruction property for bi-framelet transform). *Let $H = \{h_j\}_{j=0}^r$ and $\widetilde{H} = \{\widetilde{h}_j\}_{j=0}^r$ be two sets of finite sequences supported inside $\mathbb{Z}_M$. Then, the corresponding L-level discrete undecimal framelet transform satisfies the perfect reconstruction property if H satisfies*

Algorithm 5.2 L-level undecimal framelet transform for signals on graph

- **Decomposition**: $W_L : f \to c$
  1: **INPUT:** signal f
  2: **OUTPUT:** framelet coefficients $\{c_1^{(\ell)}, c_2^{(\ell)}, \ldots, c_r^{(\ell)}\}_{\ell=1}^{L} \cup c_0^{(L)}$
  3: Set $c_0^{(0)} = f$
  4: **for** $\ell = 1, 2, \cdots, L$ **do**
  5: $\quad c_j^{(\ell)} = W_{h_j}^{(\ell)} c_0^{(\ell-1)}, \quad$ for $0 \le j \le r$
  6: **end for**
- **Reconstruction**: $\widetilde{W}_L^* : c \to f$
  1: **INPUT:** framelet coefficients $\{c_1^{(\ell)}, c_2^{(\ell)}, \ldots, c_r^{(\ell)}\}_{\ell=1}^{L} \cup c_0^{(L)}$
  2: **OUTPUT:** signal f
  3: **for** $\ell = L-1, \cdots, 1, 0$ **do**
  4: $\quad c_0^{(\ell)} = \sum_{j=0}^{r} (W_{\widetilde{h}_j}^*)^{(\ell+1)} c_j^{(\ell+1)}$ (bi-frames), or $c_0^{(\ell)} = \sum_{j=0}^{r} (W_{h_j}^*)^{(\ell+1)} c_j^{(\ell+1)}$ (tight frame)
  5: **end for**
  6: Set $f = c_0^{(0)}$

the following conditions:

$$\sum_{j=0}^{r} \sum_{k \in \mathbb{Z}_M} \widetilde{h}_j[k] h_j^*[k-p] = \delta_p, \quad p \in \mathbb{Z}_N. \tag{5.11}$$

Proof. For the ℓ-th level decomposition, it can be seen that

$$\begin{aligned}
(W_{\widetilde{H}}^*)^{(\ell)} W_H^{(\ell)} =& \sum_{j=0}^{r} (W_{\widetilde{h}_j}^*)^{(\ell)} W_{h_j}^{(\ell)} \\
=& \sum_{j=0}^{r} \sum_{k \in \mathbb{Z}_M} \sum_{p \in \mathbb{Z}_M + k} \widetilde{h}_j[k] h_j^*[k-p] \left(\mathcal{T}_u^{(\ell)}\right)^k \left(\mathcal{T}_u^{(\ell)}\right)^{p-k} \\
=& \sum_{j=0}^{r} \sum_{p \in \mathbb{Z}_{2M}} \sum_{k \in \mathbb{Z}_M \cap (\mathbb{Z}_M + p)} \widetilde{h}_j[k] h_j^*[k-p] \left(\mathcal{T}_u^{(\ell)}\right)^k \left(\mathcal{T}_u^{(\ell)}\right)^{p-k} \\
=& s_1 + s_2 + s_3,
\end{aligned}$$

where

$$\begin{aligned}
s_1 &= \sum_{j=0}^{r} \sum_{k \in \mathbb{Z}_M} \widetilde{h}_j[k] h_j^*[k] \left(\mathcal{T}_u^{(\ell)} \left(\mathcal{T}_u^{(\ell)}\right)^{-1}\right)^k \\
s_2 &= \sum_{j=0}^{r} \sum_{p=-2M}^{-1} \sum_{k=-M}^{M+p} \widetilde{h}_j[k] h_j^*[k-p] \left(\mathcal{T}_u^{(\ell)}\right)^p \\
s_3 &= \sum_{j=0}^{r} \sum_{p=1}^{2M} \sum_{k=-M+p}^{M} \widetilde{h}_j[k] h_j^*[k-p] \left(\mathcal{T}_u^{(\ell)}\right)^p.
\end{aligned}$$

Therefore, The perfect reconstruction property (5.10) is guaranteed if $s_1 = I_N$ and $s_2 = s_3 = 0$, which leads to

$$\begin{aligned}
&\sum_{j=0}^{r}\sum_{k\in\mathbb{Z}_M} \widetilde{h}_j[k]h_j^*[k] = 1,\\
&\sum_{j=0}^{r}\sum_{k=-M}^{p+M} \widetilde{h}_j[k]h_j^*[k-p] = 0, \quad \forall p = -2M,\dots -1,\\
&\sum_{j=0}^{r}\sum_{k=p-M}^{M} \widetilde{h}_j[k]h_j^*[k-p] = 0, \quad \forall p = 1,\dots,2M.
\end{aligned}$$

Therefore, the condition (5.10) holds true if

$$\sum_{j=0}^{r}\sum_{k\in\mathbb{Z}_M} \widetilde{h}_j[k]h_j^*[k-p] = \delta_p, \quad \forall p \in \mathbb{Z}_N.$$

This completes the proof. ∎

When using the same filter bank for both decomposition and reconstruction in tight framelet transform, i.e. $H = \widetilde{H}$, we have

Corollary 5.4 (Perfect reconstruction property for tight framelet transform). *Let $H = \{h_j\}_{j=0}^r$ be one set of finite sequences supported inside $\mathbb{Z}_M$. Then, the corresponding L-level discrete undecimal tight framelet transform satisfies the perfect reconstruction property if H satisfies the following conditions:*

$$\sum_{j=0}^{r}\sum_{k\in\mathbb{Z}_M} h_j[k]h_j^*[k-p] = \delta_p, \quad p \in \mathbb{Z}_N. \tag{5.12}$$

The condition (5.12) indeed is one of the two conditions in (3.3) of the UEP for admitting MRA-based wavelet tight frames for $L^2(\mathbb{R})$. In [34, 13], a class of spline wavelet tight frames with arbitrary smoothness is constructed with explicit formulas for the associated filter banks, in which the low-pass filters h_0 are the refinement masks of B-splines with arbitrary degree.

Example 4 (B-spline filter banks [34, 13]). *The filter bank associated with linear B-spline tight frames is given by $\widetilde{H} = H$, where*

$$H = \{h_0 = \frac{1}{4}[1,2,1], \quad h_1 = \frac{1}{4}[-1,2,-1], \quad h_2 = \frac{\sqrt{2}}{4}[1,0,-1].\}$$

The filter bank associated with Cubic B-spline tight frames is given by $\widetilde{H} = H = \{h_0, h_1, h_2, h_3, h_4\}$, where $h_0 = \frac{1}{16}[1,4,6,4,1]$ and

$$\begin{aligned}
h_1 &= \tfrac{1}{16}[1,-4,6,-4,1], \quad & h_2 &= \tfrac{1}{8}[-1,2,0-2,1],\\
h_3 &= \tfrac{\sqrt{6}}{16}[1,0,-2,0,1], \quad & h_4 &= \tfrac{1}{8}[-1,-2,0,2,1].
\end{aligned}$$

We have both filter banks satisfy (5.12) and thus admit a multi-level undecimal framelet transform with perfect reconstruction property.

In the next, we give another sufficient condition on filter banks that admit tight framelet transforms with perfect reconstruction property.

PROPOSITION 5.5. *Consider a matrix $H \in \mathbb{C}^{n\times(r+1)}$. Let h_j denote the $(j+1)$-th column of H for $0 \le j \le r$. Suppose that H satisfies*

$$HH^* = \frac{1}{\sqrt{n}} I_n.$$

Then, the filter bank $\{h_0, h_1, \dots, h_r\}$ satisfies the condition (5.12).

Proof. By the condition

$$HH^* = \frac{1}{\sqrt{n}} I_n,$$

we have

$$\sum_{j=0}^{r} |h_j[k]|^2 = \frac{1}{\sqrt{n}} \quad \text{and} \quad \sum_{j=0}^{r} h_j[k] h_j^*[k'] = 0, \quad \forall k, k' \in \mathbb{Z}_M, k \neq k',$$

which leads to

$$\sum_{j=0}^{r} \sum_{k\in\mathbb{Z}_M} |h_j[k]|^2 = 1 \quad \text{and} \quad \sum_{j=0}^{r} \sum_{k\in\mathbb{Z}_M} h_j[k] h_j^*[k-p] = 0, \quad p \in \mathbb{Z}_N \backslash \{0\}.$$

Therefore, the condition (5.12) is satisfied. ∎

It can be seen from Proposition 5.5 that, as long as the filter bank forms a tight frame for $\mathbb{C}^n$ (up to a constant), we have a filter bank that admits a multi-level undecimal tight framelet transform with perfect reconstruction property.

6. Experiments and demonstrations. In this section, we demonstrate an example of discrete framelet transform on irregular graph defined in previous sections, and run the transform on some sample signals. All the experiments are conducted in MATLAB R2017b on a PC with an Intel i7 CPU and 16G memory.

6.1. Visualization of framelet transform and sparse representation of graph structured signal. Consider the graph shown in Figure 6.1, which describes the Minnesota transportation network. The graph has 2640 vertices and 6602 edges, where vertices represent road intersections, edges represent major roads, and edge weights are all equal to 1, i.e. the graph is unweighted. On such a graph, we implement discrete framelet transform associated with the Haar filter bank $H = \{\frac{1}{2}[1,1], \frac{1}{2}[1,-1]\}$ and the linear B-spline filter bank $H = \{\frac{1}{4}[1,2,1], \frac{1}{4}[-1,2,-1], \frac{\sqrt{2}}{4}[1,0,-1]\}$. See Figure 6.2 and Figure 6.3 for an illustration of scaling and wavelet functions (discrete) at different scales centered at one vertex. It can be seen that, similar to their counterparts defined on equi-spaced grid, the scaling and wavelet functions have good localization property in vertex domain, which indicates the desired capability of the resulting framelet transform on conducting local analysis of signals in vertex domain. In addition, we also show the shift operator and transit operators associated with the filters $H = \{\frac{1}{4}[1,2,1], \frac{1}{4}[-1,2,-1], \frac{\sqrt{2}}{4}[1,0,-1]\}$ in Figure 6.4.

Wavelet/framelet transform is known for its efficiency on sparse approximation to piece-wise constant signals in Euclidean space. Consider a piece-wise constant signal f defined on the Minnesota traffic graph shown in Figure 6.1, which assigns two different values to a connected region

and its complementary part in the graph. See Figure 6.7 (a) for the visualization of such a graph structured signal.

Two 3-level discrete framelet transforms are applied on such a signal: one is based on the Haar filter bank and the other is based on the linear B-spline filter bank. See Figure 6.5 and Figure 6.6 for the transform coefficients with respect to these two filter banks. It can be seen that in parallel to their counterparts on equi-spaced grids, the high-pass framelet coefficients at different scales, e.g. the coefficients indexed at $\ell = 1, 2, 3$ and $j \neq 0$ are indeed sparse. See Figure 6.7 (b) for the histogram of high-pass framelet coefficients.

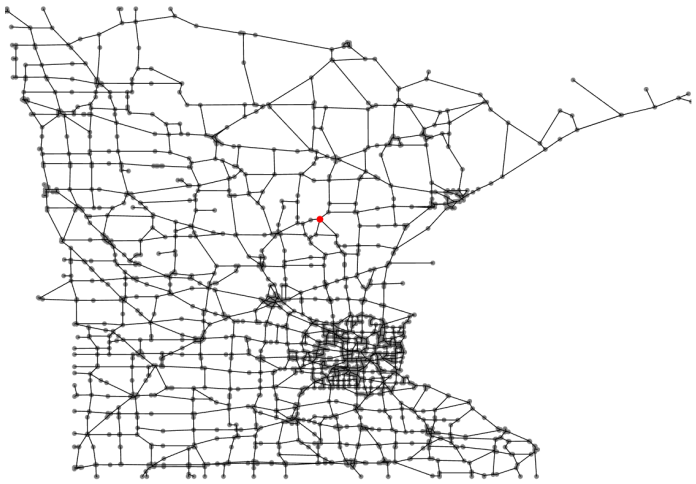

FIG. 6.1. *Minnesota traffic graph*

6.2. Robustness and efficiency of sparse approximation. In this section, an experiment is conducted to examine the reconstruction robustness, approximation efficiency and computational efficiency of sparse approximation of the proposed transform to piece-wise constant signal f shown in Figure 6.7 (a). The sparse approximation, denoted by $\widetilde{f}$, is reconstructed by only using the low-pass coefficients and the largest 25% of all high-pass framelet coefficients. Them, the approximation efficiency is measured by approximation error $\frac{\|f-\widetilde{f}\|_2}{\|f\|_2}$. See Figure 6.7 (c) for the visualization of $\widetilde{f}$. To measure the robustness of the transform. We consider that framelet coefficients of f are polluted by additive white Gaussian noise with standard deviation $\sigma = 0.1$. Then, a signal is reconstructed from such noisy coefficients, denoted by $\overline{f}$. The robustness of the transform is measured by the error $\frac{\|f-\overline{f}\|_2}{\|f\|_2}$.

The computational efficiency, robustness and approximation efficiency of the proposed framelet transform is compared to one well-known graph wavelet transform, spectral graph wavelet transform (SGWT) [19]. In the implementation of SGWT, Chebyshev polynomial approximation is used for computational efficiency. It is noted that the SGWT generates a frame not a tight frame. As a result, the reconstruction of SGWT needs to call a numerical solver for reconstruction, and the conjugate gradient method is used in their implementation. In the experiment, the stopping tolerance of the

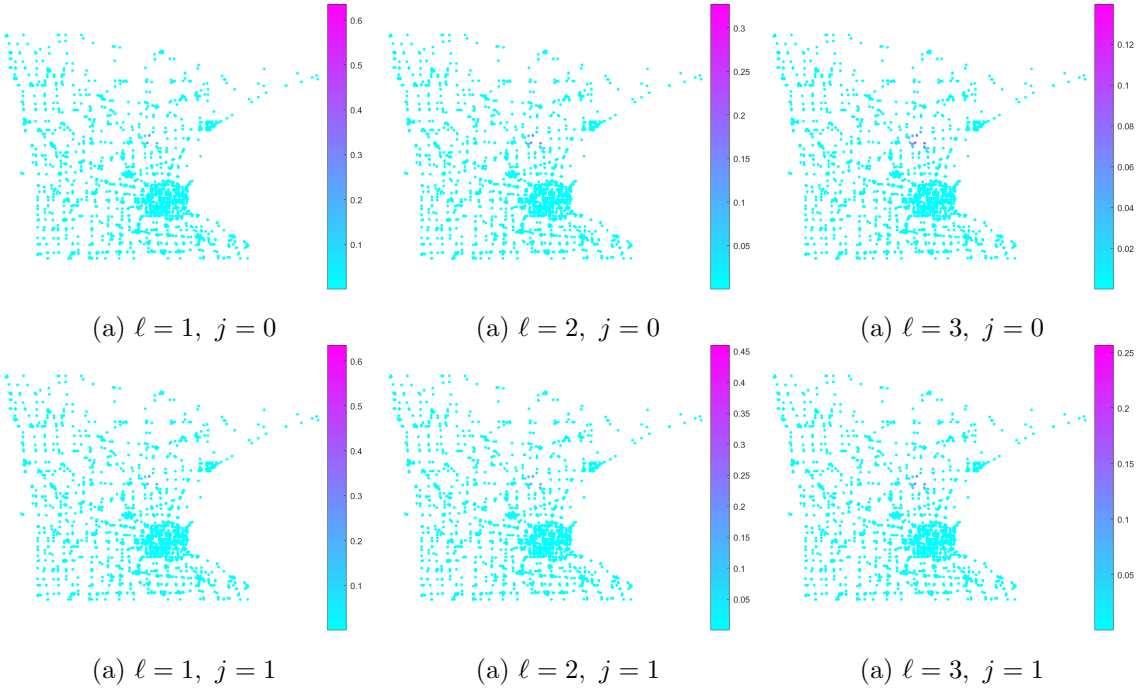

(a) $\ell = 1,\ j = 0$ (a) $\ell = 2,\ j = 0$ (a) $\ell = 3,\ j = 0$

(a) $\ell = 1,\ j = 1$ (a) $\ell = 2,\ j = 1$ (a) $\ell = 3,\ j = 1$

FIG. 6.2. *Magnitude of scaling and wavelet functions centered at a vertex (red dot in Figure 6.1(a)), with respect to the haar filter bank* $H = \{\frac{1}{2}[1,1], \frac{1}{2}[1,-1]\}$.

TABLE 6.1
Comparison of the proposed framelet transform with linear B-spline filter bank and SGWT([19]) with Chebyshev approximation for sparse approximation of the signal shown in Fig. 6.1

		Ours	SGWT-5	SGWT-10	SGWT-15
Running time (s)	Decomposition	0.0558	0.0212	0.0225	0.0251
	Reconstruction	0.0573	0.0551	0.0764	0.0816
Approximation error	Removing 75% coefficients	0.0268	0.1019	0.0234	0.0082
	Noisy coefficients ($\sigma = 0.1$)	0.1537	0.2169	0.2205	0.2259

conjugate gradient method is set as 1e-15 and the scale parameter $J = 3$. Chebyshev polynomial approximation with different polynomial orders are used in the experiments.

See Table 6.1 for the comparison between the proposed tight framelet transform and SGWT. It can be seen that when using Chebyshev approximation, the SGWT has its advantage on computational efficiency for signal decomposition. While the proposed tight framelet transform do not use any approximation scheme, it has its advantage on signal reconstruction. The main reason is that the proposed tight framelet transform forms a tight frame, and thus the reconstruction can be done by directly multiplying the transpose of the matrix associated with the decomposition operator. There is no need to solve a linear system. Indeed, it is one motivation of studying tight frame. It is expected that when processing signals of very large size, the proposed tight frame transform can be much more efficient than the SGWT on signal reconstruction.

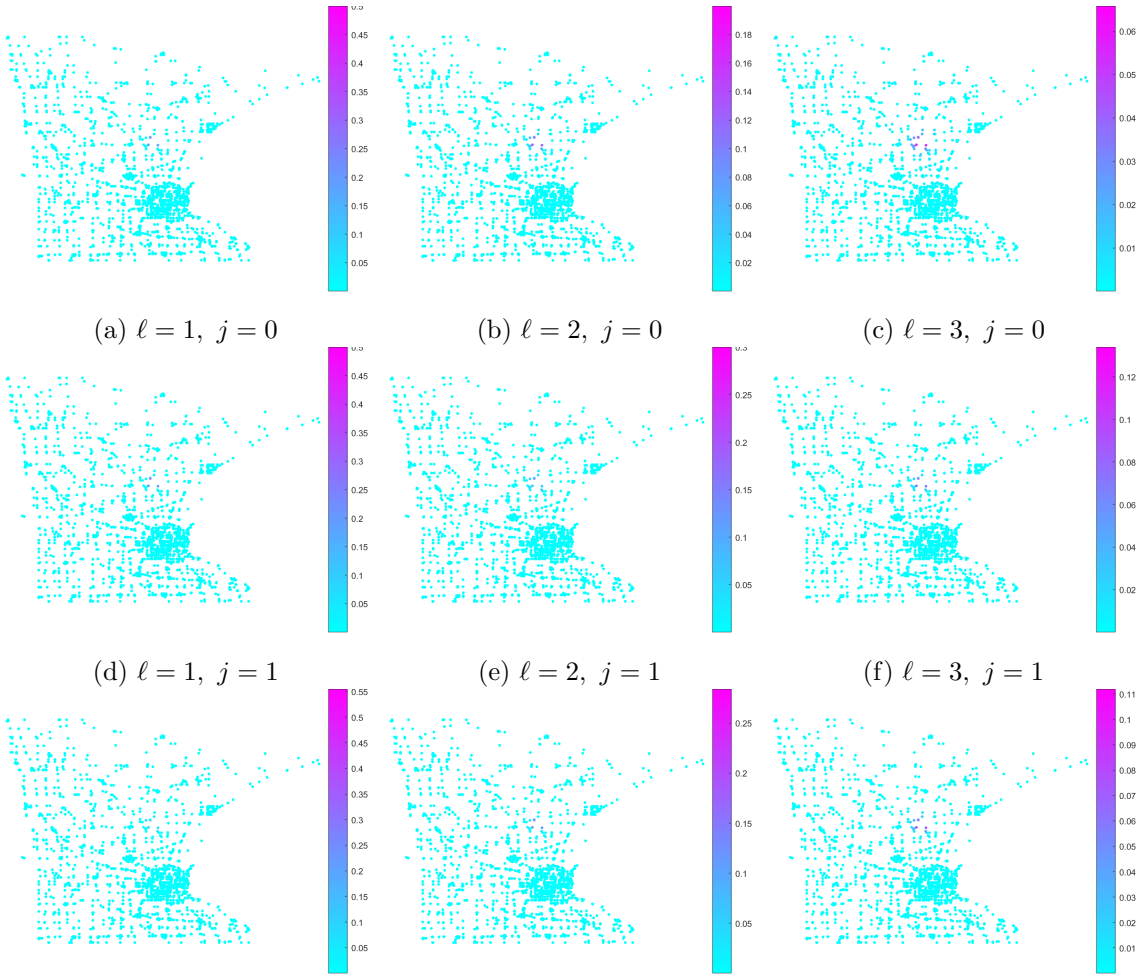

(a) $\ell = 1,\ j = 0$ (b) $\ell = 2,\ j = 0$ (c) $\ell = 3,\ j = 0$

(d) $\ell = 1,\ j = 1$ (e) $\ell = 2,\ j = 1$ (f) $\ell = 3,\ j = 1$

(g) $\ell = 1,\ j = 2$ (h) $\ell = 2,\ j = 2$ (i) $\ell = 3,\ j = 2$

FIG. 6.3. *The magnitude of scaling function and wavelet functions centered at one vertex (red dot in Figure 6.1(a)), with respect to the filter bank* $H = \{\frac{1}{4}[1,2,1], \frac{1}{4}[-1,2,-1], \frac{\sqrt{2}}{4}[1,0,-1]\}$.

Regarding the efficiency of sparse approximation, it can be seen that the proposed tight framelet transform has its advantage over SGWT with low-degree Chebyshev polynomial approximation, but loses its advantage when the degree of Chebyshev polynomial is high. Regarding the robustness, it can be seen that the proposed tight framelet transform has better robustness to noisy coefficient. Such an advantage comes from the property of tight frame, i.e., the magnitude of the eigenvalues of reconstruction matrix associated with a tight frame are either 0 or 1. In contrast, the magnitude of the eigenvalues corresponding to a frame can span a wide range, which is likely to magnify noise.

6.3. Denoising. One typical application of wavelet/framelet transform is signal denoising, which utilizes the fact that signals can sparsely approximation by framelet transform while noise

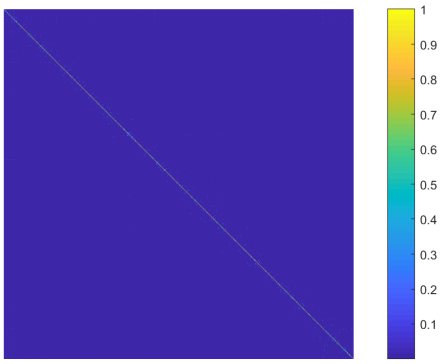

(a) shift operator: $\mathcal{T}_u^{(1)}$

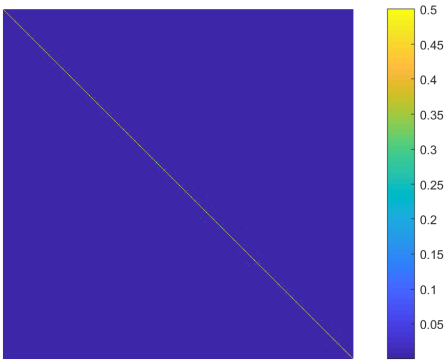

(b) transit operator $W_{h_0}^{(1)}$ with $h_0 = \frac{1}{4}[1, 2, 1]$

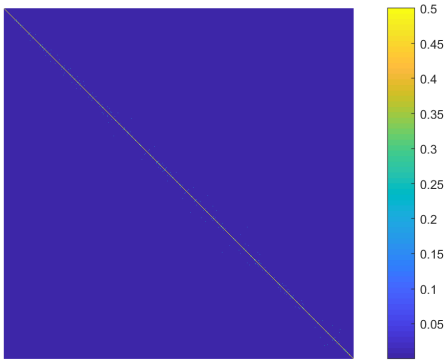

(c) transit operator $W_{h_1}^{(1)}$ with $h_1 = \frac{1}{4}[-1, 2, -1]$

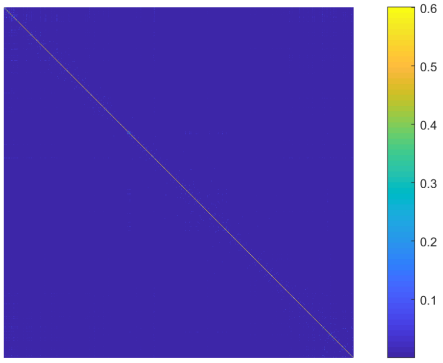

(d) transit operator $W_{h_2}^{(1)}$ with $h_2 = \frac{\sqrt{2}}{4}[1, 0, -1]\}$

FIG. 6.4. *The magnitude of shift operator and transit operations on the first level of framelet transform for the Minnesota transportation network, where the transit operators are defined from filters* $H = \{h_0 = \frac{1}{4}[1, 2, 1], h_1 \frac{1}{4}[-1, 2, -1], h_2 = \frac{\sqrt{2}}{4}[1, 0, -1]\}$.

can not. Consider the signal f shown in Fig. 6.1. Suppose the signal is polluted by additive white Gaussian noise with variance σ^2. We denoise the signal by hard thresholding method, i.e. remove those high-pass framelet coefficients with their magnitude smaller than a threshold, which is set to 0.8σ. A discrete framelet transform with B-spline filter bank of order 8 is tested in the experiment. The denoising performance on f is measured in terms of PSNR defined by

$$\text{PSNR} = 10 \log_{10} \frac{\|f\|_2^2}{\|f - \widetilde{f}\|_2^2},$$

where f and $\widetilde{f}$ denote the truth and the denoised result respectively. See Table 6.2 for the summary under different noise levels.

7. Discussion and Conclusion. In this paper, we proposed a method to construct the multi-level undecimal framelet transform for signals on undirected graph with perfect reconstruction prop-

TABLE 6.2
Results of denoising (PSNRs) by discrete framelet on graph.

σ	0.1	0.2	0.3	0.4	0.5
noisy	16.3166	10.2960	6.7742	4.2754	2.3372
denoised	18.8128	14.9627	12.7456	10.9598	9.4915

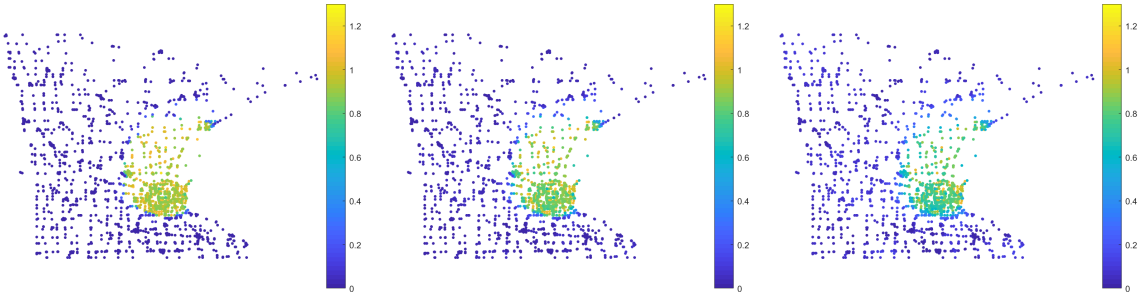

(a) $\ell = 1,\ j = 0$ (a) $\ell = 2,\ j = 0$ (a) $\ell = 3,\ j = 0$

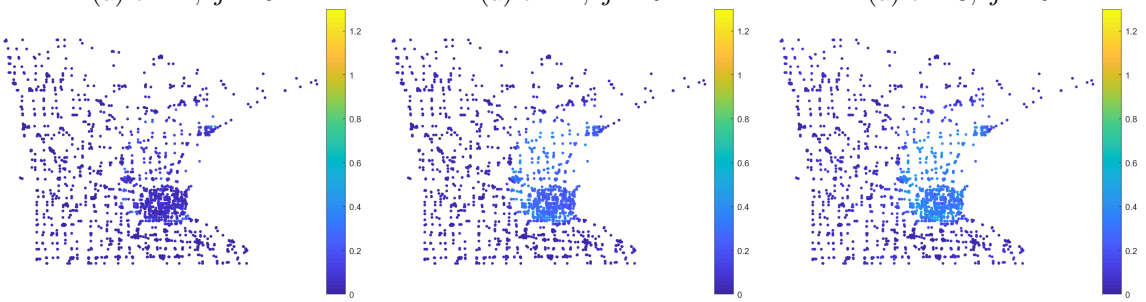

(a) $\ell = 1,\ j = 1$ (a) $\ell = 2,\ j = 1$ (a) $\ell = 3,\ j = 1$

FIG. 6.5. *The magnitude of framelet coefficients of piece-wise constant signals shown in Figure 6.1 (b), with respect to the Haar filter bank* $H = \{\frac{1}{2}[1,1], \frac{1}{2}[1,-1]\}$.

erty. By defining basic blocks of framelet transform with strong motivation from its counterparts for equi-spaced grids, including shift, convolution and up/down sampling, we have a painless construction scheme of multi-level framelet transform whose associated filter bank can directly call those associated with existing classic wavelet bi-frames and tight frames. The discrete framelet transform constructed in this paper for graph keeps most desired properties of classic framelet transform, e.g., perfect reconstruction property and efficient sparse approximation to piece-wise constant signals, which makes it an appealing tool for processing and analyzing graph-structured signals.

Acknowledgement.

REFERENCES

[1] J. C. BREMER, R. R. COIFMAN, M. MAGGIONI, AND A. D. SZLAM, *Diffusion wavelet packets*, Appl. Comput. Harmon. Anal., 21 (2006), pp. 95–112.
[2] J.-F. CAI, R. CHAN, AND Z. SHEN, *A framelet-based image inpainting algorithm*, Appl. Comput. Harmon.

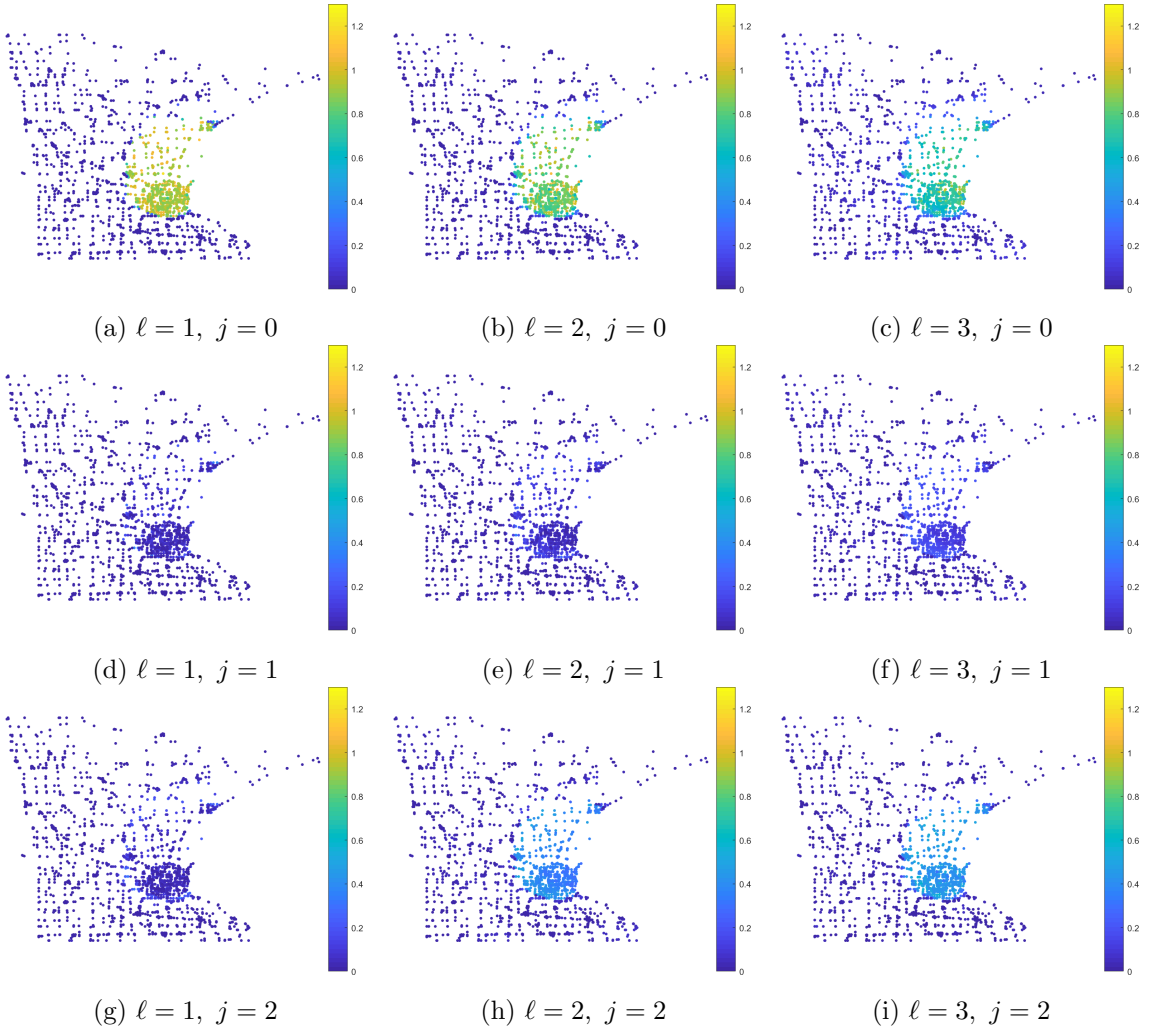

(a) $\ell = 1,\ j = 0$ (b) $\ell = 2,\ j = 0$ (c) $\ell = 3,\ j = 0$

(d) $\ell = 1,\ j = 1$ (e) $\ell = 2,\ j = 1$ (f) $\ell = 3,\ j = 1$

(g) $\ell = 1,\ j = 2$ (h) $\ell = 2,\ j = 2$ (i) $\ell = 3,\ j = 2$

FIG. 6.6. *The magnitude of framelet coefficients of the piece-wise constant signal shown in Figure 6.1 (b), with respect to the linear B-spline filter bank* $H = \{\frac{1}{4}[1,2,1], \frac{1}{4}[-1,2,-1], \frac{\sqrt{2}}{4}[1,0,-1]\}$.

Anal., 24 (2008), pp. 131–149.

[3] J.-F. CAI, H. JI, C. LIU, AND Z. SHEN, *Framelet based blind image deblurring from a single image*, IEEE Trans. Image Proc., 21 (2012), pp. 562–572.

[4] J.-F. CAI, H. JI, Z. SHEN, AND G. B. YE, *Data-driven tight frame construction and image denoising*, Appl. Comput. Harmon. Anal., 37 (2014), pp. 89–105.

[5] Y. H. CHAO, A. ORTEGA, W. HU, AND G. CHEUNG, *Edge-adaptive depth map coding with lifting transform on graphs*, in 2015 Picture Coding Symposium, 2015, pp. 60–64.

[6] C. CHUI, F. FILBIR, AND H. MHASKAR, *Representation of functions on big data: graphs and trees*, Appl. Comput. Harmon. Anal., 38 (2015), pp. 489–509.

[7] C. K. CHUI, H. MHASKAR, AND X. ZHUANG, *Representation of functions on big data associated with directed graphs*, Appl. Comput. Harmon. Anal., 44 (2018), pp. 165–188.

[8] F. R. CHUNG, *Spectral graph theory*, vol. 92, American Mathematical Soc., 1997.

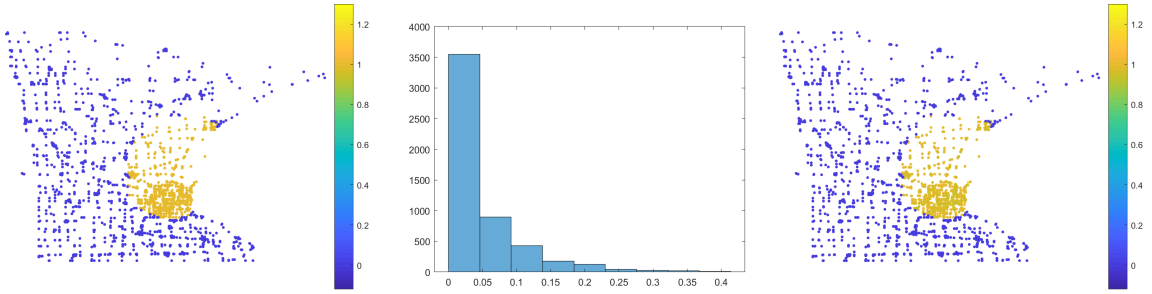

(a) original function (b) histogram of high-pass coefficients (c) reconstructed function

FIG. 6.7. *The piece-wise constant function defined on the graph, and the reconstruction using partial coefficients of framelet transform associated with linear spline filter bank* $H = \{\frac{1}{4}[1,2,1], \frac{1}{4}[-1,2,-1], \frac{\sqrt{2}}{4}[1,0,-1]\}$. *The coefficients used for reconstruction include all low-pass coefficients and top 25% (in magnitude) high-pass coefficients.*

[9] R. COIFMAN AND D. DONOHO, *Translation-invariant de-noising*, in Wavelet and Statistics, vol. 103 of Springer Lecture Notes in Statistics, Springer-Verlag., 1994, pp. 125–150.

[10] R. R. COIFMAN AND M. MAGGIONI, *Diffusion wavelets*, Appl. Comput. Harmon. Anal., 21 (2006), pp. 53–94.

[11] M. CROVELLA AND E. KOLACZYK, *Graph wavelets for spatial traffic analysis*, in Proc. of INFOCOM, vol. 3, IEEE, 2003, pp. 1848–1857.

[12] I. DAUBECHIES, *Ten lectures on wavelets*, vol. 61, SIAM, 1992.

[13] I. DAUBECHIES, B. HAN, A. RON, AND Z. SHEN, *Framelets: MRA-based constructions of wavelet frames*, Appl. Comput. Harmon. Anal., 14 (2003), pp. 1–46.

[14] B. DONG, *Sparse representation on graphs by tight wavelet frames and applications*, Appl. Comput. Harmon. Anal., 42 (2017), pp. 452–479.

[15] B. DONG AND Z. SHEN, *Mra-based wavelet frames and applications*, in IAS/Park City Mathematics Series: The Mathematics of Image Processing, vol. 19, 2010, pp. 7–185.

[16] V. N. EKAMBARAM, G. C. FANTI, B. AYAZIFAR, AND K. RAMCHANDRAN, *Spline-like wavelet filterbanks for multiresolution analysis of graph-structured data*, IEEE Trans. Signal Inf. Process. Netw., 1 (2015), pp. 268–278.

[17] Z. FAN, A. HEINECKE, , AND Z. SHEN, *Duality for frames*, J. Fourier Anal. Appl., (2015).

[18] M. GAVISH, B. NADLER, AND R. R. COIFMAN, *Multiscale wavelets on trees, graphs and high dimensional data: Theory and applications to semi supervised learning*, in ICML, 2010, pp. 367–374.

[19] D. K. HAMMOND, P. VANDERGHEYNST, AND R. GRIBONVAL, *Wavelets on graphs via spectral graph theory*, Appl. Comput. Harmon. Anal., 30 (2011), pp. 129–150.

[20] N. LEONARDI AND D. V. D VILLE, *Wavelet frames on graphs defined by fmri functional connectivity*, in IEEE International Symposium on Biomedical Imaging: From Nano to Macro, 2011, pp. 2136–2139.

[21] N. LEONARDI AND D. V. D. VILLE, *Tight wavelet frames on multislice graphs*, IEEE Trans. Signal Process., 61 (2013), pp. 3357–3367.

[22] M. LI, Z. FAN, H. JI, AND Z. SHEN, *Wavelet frame based algorithm for 3d reconstruction in electron microscopy*, SIAM J. Sci. Comput., 36 (2014), pp. 45–69.

[23] M. MAGGIONI, J. C. BREMER, R. R. COIFMAN, AND A. D. SZLAM, *Biorthogonal diffusion wavelets for multiscale representations on manifolds and graphs*, in Wavelets XI, vol. 5914, International Society for Optics and Photonics, 2005, p. 59141M.

[24] S. MALLAT, *A Wavelet Tour of Signal Processing, Third Edition: The Sparse Way*, Academic Press, San Diego, CA, 2008.

[25] E. MARTINEZ-ENRIQUEZ, F. DIAZ-DE-MARIA, AND A. ORTEGA, *Video encoder based on lifting transforms on graphs*, in 2011 18th IEEE International Conference on Image Processing, 2011, pp. 3509–3512.

[26] E. MARTINEZ-ENRIQUEZ AND A. ORTEGA, *Lifting transforms on graphs for video coding*, in Data Compression Conference, 03 2011, pp. 73–82.

[27] S. K. NARANG, Y. H. CHAO, AND A. ORTEGA, *Critically sampled graph based wavelet transforms for image coding*, in 2013 Asia Pacific Signal and Information Processing Association Annual Summit and Conference, 2013, pp. 1–4.

[28] S. K. Narang and A. Ortega, *Lifting based wavelet transforms on graphs*, in APSIPA ASC, 2009, pp. 441–444.
[29] S. K. Narang and A. Ortega, *Perfect reconstruction two-channel wavelet filter banks for graph structured data*, IEEE Trans. Signal Process., 60 (2012), pp. 2786–2799.
[30] J. D. Power, A. L. Cohen, S. M. Nelson, G. S. Wig, K. A. Barnes, J. A. Church, A. C. Vogel, T. O. Laumann, F. M. Miezin, B. L. Schlaggar, et al., *Functional network organization of the human brain*, Neuron, 72 (2011), pp. 665–678.
[31] I. Ram, M. Elad, and I. Cohen, *Generalized tree-based wavelet transform*, IEEE Trans. Signal Process., 59 (2011), pp. 4199–4209.
[32] I. Ram, M. Elad, and I. Cohen, *Redundant wavelets on graphs and high dimensional data clouds*, IEEE Signal Process. Lett., 19 (2012), pp. 291–294.
[33] A. Ron and Z. Shen, *Affine system in $L_2(R^d)$: the analysis of the analysis operator*, J. Funct. Anal., 148 (1997).
[34] A. Ron and Z. Shen, *Affine systems in $L_2(R^d)$ ii: Dual systems*, J. Fourier Anal. Appl., 3 (1997), pp. 617–637.
[35] A. Sakiyama, K. Watanabe, Y. Tanaka, and A. Ortega, *Two-channel critically sampled graph filter banks with spectral domain sampling*, IEEE Trans. Signal Process., 67 (2019), pp. 1447–1460.
[36] A. Sandryhaila and J. M. Moura, *Discrete signal processing on graphs*, IEEE Trans. Signal Process., 61 (2013), pp. 1644–1656.
[37] A. Sandryhaila and J. M. Moura, *Discrete signal processing on graphs: Graph fourier transform.*, in ICASSP, 2013, pp. 6167–6170.
[38] A. Sandryhaila and J. M. Moura, *Big Data Analysis with Signal Processing on Graphs: Representation and processing of massive data sets with irregular structure*, IEEE Signal Process. Mag., 31 (2014), pp. 80–90.
[39] A. Sandryhaila and J. M. Moura, *Discrete signal processing on graphs: Frequency analysis.*, IEEE Trans. Signal Process., 62 (2014), pp. 3042–3054.
[40] G. Shen and A. Ortega, *Optimized distributed 2d transforms for irregularly sampled sensor network grids using wavelet lifting*, in ICASSP, IEEE, 2008, pp. 2513–2516.
[41] G. Shen and A. Ortega, *Transform-based distributed data gathering*, IEEE Trans. Signal Process., 58 (2010), pp. 3802–3815.
[42] Z. Shen, *Wavelet frames and image restorations*, in Proc. ICM, vol. 4, Hindustan Book Agency, India, 2010, pp. 2834–2863.
[43] D. I. Shuman, C. Eiesmeyr, N. Holighaus, and P. Vandergheynst, *Spectrum-adapted tight graph wavelet and vertex-frequency frames*, IEEE Trans. Signal Process., 63 (2015), pp. 4223–4235.
[44] D. I. Shuman, M. Faraji, and P. Vandergheynst, *Semi-supervised learning with spectral graph wavelets*, in International Conference on Sampling Theory and Applications, 2011, pp. 2136–2139.
[45] M. Tan and A. Qiu, *Spectral Laplace-Beltrami wavelets with applications in medical images*, IEEE Trans. on Med. Imaging, 34 (2015), pp. 1005–1017.